

Numerical investigations on ergodicity of solute transport in heterogeneous aquifers

N. Suci¹, C. Vamoș², J. Vanderborght³, H. Hardelauf³, and H. Vereecken³

Received 31 August 2005; revised 10 December 2005; accepted 17 January 2006; published 18 April 2006.

[1] Darcy velocities for lognormal hydraulic conductivity with small variance and finite correlation length were approximated by periodic random fields. Accurate simulations of two-dimensional advection-dispersion processes were achieved with the global random walk algorithm, using 10^{10} particles in every transport realization. Reliable statistical estimations were obtained by averaging over 256 realizations. The main result is a numerical evidence for the mean square convergence of the actual concentrations to the macrodispersion process predicted by a known limit theorem. For small initial plumes the ergodic behavior can be expected after thousands of advection timescales, when the deviation from the theoretical prediction of the cross-section space-averaged concentration monotonously decays and falls under 20%. The increase of the transverse dimension of the initial plume slows down the approach to the quasi-ergodic state and has a nonlinear effect on the variability of the actual concentrations and dispersivities.

Citation: Suci¹, C. Vamoș², J. Vanderborght³, H. Hardelauf³, and H. Vereecken³ (2006), Numerical investigations on ergodicity of solute transport in heterogeneous aquifers, *Water Resour. Res.*, 42, W04409, doi:10.1029/2005WR004546.

1. Introduction

[2] It is generally admitted that groundwater quality is mainly affected by the transport of dissolved chemicals through soils and aquifers. The classical model is based on a dispersion and advection mechanism which describes the transport at some “local scale.” Further, one assumes that the variability of the solute movement in subsurface water is caused by the heterogeneity of the hydraulic conductivity which, for a given natural formation, is efficiently described as a realization of a random space function [Sposito *et al.*, 1986; Hassan *et al.*, 1998]. The corresponding advection velocity field becomes a random function also and the transport in natural porous media is described by a stochastic model [Dagan, 1984] which follows the approach for turbulent diffusion in atmosphere [Taylor, 1921], or, in terms of the mathematical theory of stochastic processes, as a diffusion in a random velocity field [Matheron and de Marsily, 1980; Avellaneda and Majda, 1992].

[3] As shown by Sposito *et al.* [1986], once the advection-dispersion model for local scale has been inferred, the stochastic modeling of transport in groundwater consists of two successive steps. First, the behavior of the ensemble averaged concentration has to be investigated to look for the existence of an upscaled diffusive behavior called “macrodispersion.” The second issue is to assess the applicability of the ensemble statistics to predictions made for a single groundwater system. The latter, which is the central prob-

lem in stochastic modeling, is generally referred to as “ergodicity” in hydrogeological literature [Dagan, 1984, 1987; Kabala and Sposito, 1994; Sposito, 1997; Fiori, 1998; Trefry *et al.*, 2003; Janković *et al.*, 2003]. It is in this sense that the term ergodicity will be used in the following.

[4] Even though abundant literature has been produced in the last two decades, the investigations on ergodicity were in most cases limited to the study of the second moments of the solute plume and the conclusions often disagree. For instance, it is accepted that the length scale to reach the asymptotic limit predicted by the stochastic model is impractical for real contamination problems [Berkowitz, 2001; Schwarze *et al.*, 2001; Dentz *et al.*, 2002, 2003; Eberhard, 2004]. However, recent numerical investigations conclude that, for extended initial plumes, the dispersivities behave ergodically, at relatively small distances from the injection domain [Janković *et al.*, 2003]. These conclusions do not agree with the results of Trefry *et al.* [2003], which show that the dispersivities significantly differ from realization to realization even after hundreds of heterogeneity scales and the concentrations do not reach the Gaussian limit predicted by the stochastic macrodispersion model. The result of Trefry *et al.* [2003] is consistent with other numerical simulations which show that the attainment of a quasi-ergodic state is more complicated than indicated by some analytical approaches [Naff *et al.*, 1998b].

[5] To examine whether, when and how accurately the stochastic model predicts the behavior in actual aquifers, we propose numerical quantitative estimations of the quasi-ergodic behavior in the spirit of the “operational ergodicity” of Kabala and Sposito [1994]. We use a rigorous mathematical proof of the existence of the upscaled macrodispersion process to check whether the numerical method is accurate enough for our purpose. Further, we use the same theoretical result to investigate the ergodicity. That is to say, we are looking for those indicators of the contam-

¹Institute of Applied Mathematics, Friedrich-Alexander University of Erlangen-Nuremberg, Erlangen, Germany.

²“T. Popoviciu” Institute of Numerical Analysis, Romanian Academy, Cluj-Napoca, Romania.

³Institute of Agrosphere (ICG-IV), Research Center Jülich, Jülich, Germany.

ination in actual plumes that can be predicted by the theoretical result, in the limits of acceptable errors. The numerical task is carried out with the “global random walk” algorithm (GRW) [Vamoş *et al.*, 2003]. Superseding the limitations encountered by the classical particle tracking method, the GRW algorithm performs the simulation of advection-dispersion displacements over thousands of advection timescales of tens of billions of particles, initially distributed over hundreds of heterogeneity scales.

[6] For the sake of clarity and for computational reasons, we consider only the classical stochastic model, two-dimensional transport problems and small variance of the velocity field in our numerical investigations. This permits detailed analyses of transport in velocity fields with finite correlation lengths, which are not possible in less restrictive conditions. In the following we discuss these limitations and present some reasons to choose this methodological frame.

[7] More recently, stochastic models free of the Fickian hypothesis were proposed as alternatives to the classical stochastic model. These models generally describe ensemble averaged concentrations and their parameters can, in principle, be derived from measurable properties of the medium (breakthrough curves or hydraulic conductivities). The theory proposed by Cushman and Moroni [2001] generalizes the statistical mechanical approach for Hamiltonian systems to an arbitrary statistical ensemble with invariant probability measure and it enables the description of anomalous dispersion induced by velocity fluctuations evolving over a hierarchy of scales on the scale of observation. Berkowitz and Scher [2001] presented a general approach, based on the ensemble average of a master equation, equivalent to a continuous time random walk over a range of length scales on which the statistical homogeneity can be assumed. This approach was extended to a Fokker-Planck equation with memory term, which integrates the transport behavior over homogeneous units of the medium, each of them described by the ensemble averaged master equation [Cortis *et al.*, 2004]. Another promising stochastic model for transport in saturated porous media describes the trajectories of the solute particles, in the position-velocity phase space, by means of a Langevin stochastic differential equation which accounts for non-Fickian features of the transport as well [Kurbanmuradov *et al.*, 2003]. The ensemble average of the classical advection-dispersion equations can be obtained under appropriate limiting conditions as particular cases of the three stochastic models mentioned above.

[8] The classical model is also able to capture the complexity of transport in groundwater. Anomalous diffusion in the preasymptotic transport regime presumably occurs under quite broad conditions [Trefry *et al.*, 2003]. For more restrictive conditions (perfectly stratified aquifers), the ensemble averaged solution of the classical model can be superdiffusive at all times [Matheron and de Marsily, 1980]. However, what really makes the classical model attractive for applications is the existence of mathematical proofs for the diffusive behavior of the ensemble averaged concentration, for typical groundwater transport problems, characterized by velocity fields with finite correlations lengths. Since the classical model describes the transport in given velocity fields, the quantitative approach to ergodicity is straightforward and consists in analyzing the

sample-to-sample fluctuations and the deviation of the ensemble averaged solutions from the macrodispersion process. Therefore, in the following we consider only the model based on the advection-dispersion mechanism. The conclusions of such an investigation could be useful in assessing the predictive power of the stochastic modeling which does not assume the Fickian behavior at a local scale.

[9] Two-dimensional models can be very useful tools to predict contamination in natural aquifers [Hassan *et al.*, 1998]. They may be applied to the case of hydraulic conductivity which is isotropic in the horizontal plane but has a much smaller correlation length in the vertical direction as well as to transport at regional scale [Dagan, 1987]. Two-dimensional numerical simulations in vertical planes oriented along the mean flow direction were successful in reproducing the experimental results obtained in tracer tests [Moltyaner *et al.*, 1993]. The two-dimensional simulations also provide insight into the convergence of the transport process to the Gaussian limit [Trefry *et al.*, 2003]. This is mainly relevant when ergodicity is investigated, as suggested by Dagan [1984, 1987], through averages over space domains with large transverse dimensions. Then, the behavior of the space mean concentration is mainly governed by the longitudinal dispersivities which tend in ensemble mean to the same limit and are quite close after a few tens of heterogeneity scales, for both two- and three-dimensional transport in aquifers with moderate variability of the hydraulic conductivity [Dagan, 1987; Fiori *et al.*, 2003; Dentz *et al.*, 2002, 2003].

[10] The presumption that the hydraulic conductivity has a lognormal distribution and small variance is an accepted simplification leading to Gaussian velocity fields which can capture the essential features of the stochastic model [Cortis *et al.*, 2004; Eberhard, 2004]. In the present context, this choice is not a limitation since the existence of the upscaled Gaussian distribution for the ensemble averaged concentration, used as reference in our investigations, is ensured for Gaussian velocity fields when the velocity variance goes to zero.

[11] The paper is structured as follows. Section 2 contains some definitions and results concerning the notions of macrodispersion and ergodicity. Section 3 contains some general considerations on numerical modeling as well as the statement of our numerical method. Section 4 presents the main numerical results. Conclusions are drawn in section 5. Appendix A presents the GRW algorithm and details on the numerical computations. Appendix B is dedicated to technical details concerning the transport problem which approximately fulfils the theoretical requirements for the existence of upscaled Gaussian diffusion and to the statistics of numerically generated velocity fields.

2. Macrodispersion and Ergodicity

2.1. Macrodispersion Stochastic Model

[12] For slowly variable porosity which can be taken as a constant, and for nonreactive solutes, the mathematical model of transport in saturated porous media is given by an advection-dispersion equation for the concentration field $c(\mathbf{x}, t)$,

$$\partial_t c + \mathbf{V} \nabla c = \mathbf{D} \nabla^2 c. \quad (1)$$

The constant “local dispersion coefficient” \mathbf{D} accounts for both the molecular diffusion and the hydrodynamic mixing due to the small-scale variability of the velocity field [Sposito *et al.*, 1986; Kapoor and Gelhar, 1994; Labolle and Fogg, 2001; Janković *et al.*, 2003]. The stochastic approach considers stationary velocities $\mathbf{V}(\mathbf{x})$ which are realizations of a random field (random space function) that is statistically homogeneous.

[13] A stochastic process has “diffusive behavior” when the mean squared displacement, or variance, is linear as function of time. The typical example is the Brownian motion, i.e., the one-dimensional Gaussian process $X(t)$ with zero mean and variance $\sigma^2(t) = \langle X^2 \rangle(t) = 2Dt$. In this case, the diffusion coefficient D describes both the shape of the Gaussian distribution and the width of the diffusion front $\langle X^2 \rangle$. In the case of the process described by the equation (1), and, generally, in systems with space-time variable properties, the width of the diffusion fronts is no longer given by the diffusion coefficients alone. Instead, the rate of increase of the second centered moment $\sigma^2(t)$ defines “effective diffusion coefficients”

$$\mathbf{D}^{\text{eff}}(t) = \frac{\sigma^2(t)}{2t}, \quad (2)$$

which can be used to check whether the process has a diffusive behavior [Avellaneda and Majda, 1992]. The existence of a constant limit for $t \rightarrow \infty$ of the effective coefficients (2) is ensured, for every realization of the velocity field, by some weak conditions on the partial derivatives of \mathbf{V} (bounded vector potential) [Avellaneda and Majda, 1989; Tatarinova *et al.*, 1991].

[14] The definition (2) was mainly used in hydrological applications for comparisons between theory and field tests [Dagan, 1987] and to compute the first-order approximations of dispersivities by traveltime statistics [Vanderborght and Vereecken, 2002; Fernández-García *et al.*, 2005a, 2005b]. Sometimes, in analytical approaches [Attinger *et al.*, 1999; Dentz *et al.*, 2000a] or numerical studies [Tompson and Gelhar, 1990; Trefry *et al.*, 2003] the dispersion is described by the local slope, $d\sigma^2/dt$ or by the mean slope of the variance

$$\tilde{\mathbf{D}}(t) = \frac{\sigma^2(t) - \sigma^2(0)}{2t} = \mathbf{D}^{\text{eff}}(t) - \frac{\sigma^2(0)}{2t}. \quad (3)$$

At large times $\tilde{\mathbf{D}}$ tends to \mathbf{D}^{eff} and the slope of the variance can be used as well to define the asymptotic effective coefficients. However, the time behavior of the solute plume is properly described by the rate of increase of the second moment (2), which, unlike the mean slope (3), is positive-definite at all times.

[15] Since disconnected, bimodal or asymmetric plumes could have the same second moment as a Gaussian plume, the existence of the coefficients (2) do not yet prove the existence of the Gaussian limit process. A limit theorem was demonstrated by Kesten and Papanicolaou [1979]. Neglecting the local dispersion in (1), considering velocity fields with nonvanishing mean \mathbf{U} and small fluctuations $\varepsilon\mathbf{u}$, $\varepsilon \ll 1$, $\mathbf{V} = \mathbf{U} + \varepsilon\mathbf{u}$, and making the assumption that the field has some “strong mixing” property, as characterized by a suitable fast decay of the correlation function $\mathbf{r}(\mathbf{x})/\varepsilon^2 =$

$\langle \mathbf{u}(\mathbf{0})\mathbf{u}(\mathbf{x}) \rangle$, the authors proved that the average of the transport process over the realizations of the velocity field can be upscaled to a Gaussian diffusion. In the “weakly random limit” ($\varepsilon \rightarrow 0$, $t \rightarrow \infty$, $\varepsilon^2 t = \text{constant}$), the ensemble averaged concentration verifies an advection-diffusion equation with the upscaled diffusion coefficients given by

$$\mathbf{D}^* = \int_0^\infty \mathbf{r}(\mathbf{U}t) dt.$$

Under these conditions, Taylor’s [1921] statement gets a rigorous proof.

[16] Using a scaling argument, Winter *et al.* [1984] show that when the local coefficients \mathbf{D} are of the order ε^2 , an extension of the exact result of Kesten and Papanicolaou [1979] to advection-diffusion processes is possible and the upscaled diffusion coefficients are of the form

$$\mathbf{D}^* = \mathbf{D} + \int_0^\infty \mathbf{r}(\mathbf{U}t) dt. \quad (4)$$

For incompressible velocity fields, the upscaled velocity equals the mean velocity \mathbf{U} . We remark here that the upscaled coefficient (4) has the same form as the first-order approximation of the “macrodispersion coefficient” derived by Dagan [1984]. A test for the accuracy of our numerical simulations which mimic the above conditions is to check whether the deviations of the computed upscaled coefficients from the theoretical values given by (4) are one order of magnitude smaller than the local dispersion coefficient.

2.2. Ergodicity

[17] Strictly speaking, the macrodispersion model is directly applicable to a single aquifer if the same asymptotic Gaussian approximation holds for each realization [Sposito *et al.*, 1986]. Hereafter we call this strong property “asymptotic ergodicity.” Sufficient conditions for asymptotic ergodicity are provided if the ensemble average of the actual concentrations tend to the solution of the macrodispersion model and the sample-to-sample fluctuations tend to zero. In this case, the effective coefficients in every realization necessarily also tend to the macrodispersion coefficients.

[18] The assumption underlying the concept of ergodicity is that suitable space averages of the actual concentration can be described by the solution of the macrodispersion model, when the spatial variability of the concentration encompasses the variability from realization to realization. Dagan [1984, 1987] assumed that the space and the ensemble mean are interchangeable if the variance of the space averaged concentration tends to zero. It was shown that the spatially averaged concentration in single realizations is close to the macrodispersion solution after tens of correlation lengths of the hydraulic conductivity, if the initial solute body or the domain of the space average extends over a few correlation lengths across the mean flow [Dagan, 1984, p. 165]. This result was derived in a Lagrangian frame for a normal distribution of the displacements of the solute particles, inferred by a first-order approximation of the transport equations. A similar approach, using another approximation technique [Dagan, 1987, equation (3.14)], led however to a different result indicating a nonergodic behavior, manifested by a finite

limit of the concentration fluctuations at the plume center of mass, which is practically reached after a few correlation lengths [Dagan and Fiori, 1997, Figure 3]. The same approximation led to a finite asymptotic variance of the longitudinal second moment of the plume [Fiori, 1998, Figures 4 and 5], which also indicates nonergodic behavior. These results contradict other Lagrangian approaches [Pannone and Kitanidis, 1999] and Eulerian theories (which are limited in turn by closure approximations) [Kapoor and Gelhar, 1994; Kapoor and Kitanidis, 1998]. A renewed Lagrangian result of Fiori and Dagan [2000] corrects the previous one, showing that the concentration coefficient of variation tends to zero (after much larger traveltimes, corresponding to thousands of correlation scales) but predicts a large time behavior which is still different from that obtained in Eulerian approaches.

[19] The ergodic behavior of individual plumes was recently investigated numerically. Janković *et al.* [2003] found a good agreement between the behavior of the individual plumes and the predictions of the macrodispersion model, for both two- and three-dimensional transport simulations, which suggests an ergodic behavior of the extended plumes as predicted by Dagan [1984]. On the contrary, Trefry *et al.* [2003], who simulated the concentration field in single realizations of transport for two-dimensional plumes with initial extension of tens of correlation lengths across the mean flow, found that the ergodic behavior is not reached even when the plumes have traveled hundreds of correlations lengths. The last result is apparently in agreement with that found by Fiori and Dagan [2000]. Yet, the two numerical approaches are not completely comparable. Trefry *et al.* [2003] performed a direct investigation, by comparing the dispersivities in given realizations, defined by the effective coefficients (3) divided by the mean velocity, to the macrodispersivities corresponding to the upscaled coefficients (4) of the stochastic model. They also checked whether the concentration becomes Gaussian. Janković *et al.* [2003] did not investigate the concentration field and in their paper the macrodispersivities were computed through a Taylor formula, similar to (4) [see Janković *et al.*, 2003, equation (14)] which gives smoother results and can explain the different conclusions in the two papers.

[20] In spite of the common belief that extended initial plumes have an ergodic behavior, there are no general mathematical proofs for that. The relevance of the macrodispersion model for a single realization of the medium is not an immediate consequence of the existence of the Gaussian upscaling and is not ensured either by the ergodic properties of the random velocity field [Sposito *et al.*, 1986; Kabala and Sposito, 1994]. Moreover, in the limiting case of vanishing local dispersion, it was proved that groundwater flows governed by the Darcy law are geometrically constrained against becoming chaotic and, consequently, the purely advective transport is in general not ergodic [Sposito, 1997, 2001]. The stratified aquifer model of Matheron and de Marsily [1980] provides another counter example, for the complete advection-dispersion model. The exact expressions derived by Clincy and Kinzelbach [2001] show that the fluctuations of the longitudinal effective coefficient tend to a finite limit, even if the flow is not aligned with the strata and the transport has asymptotic

diffusive behavior. Since the asymptotic effective coefficients in given realizations do not tend to their expectation (a necessary condition for ergodicity), the transport is not ergodic. Quantitative numerical estimations for the deviation from the macrodispersion model of the transport in realizations of a Gaussian velocity field with finite correlation lengths (in both transverse and longitudinal directions) were recently obtained, for the case of point-like initial plumes [Eberhard, 2004]. The numerical computations of Eberhard [2004], based on approximate solutions of the transport equation, show that the fluctuations of the longitudinal effective coefficient tend to zero, indicating that a necessary condition for ergodicity is fulfilled. To prove the ergodicity of transport in velocity fields with finite correlation lengths it is necessary to check whether the sufficient conditions, formulated for actual concentrations, are verified. It is also useful to investigate the behavior of the effective coefficients for extended plumes and their relation with ergodicity.

[21] To achieve our goals, we introduce a definition which is general enough to include various conceptual features of the term ergodicity cited above. Let $A(t)$ be the value of an observable at time t , $A^*(t)$ the theoretical prediction and $\Delta A = \langle (A - A^*)^2 \rangle^{1/2}$ the root mean square deviation from theory (the angular brackets denote averaging over the ensemble of realizations of the velocity field). The observable A is ergodic within the range η , $\eta > 0$, if $\Delta A \leq \eta$. Since the theory usually predicts A^* as an asymptotic limit and the observable A is known at finite times, in practice a more flexible definition is necessary. From the relation $(\Delta A)^2 = \sigma_A^2 + (\Delta \langle A \rangle)^2$, where $\sigma_A = \langle (A - \langle A \rangle)^2 \rangle^{1/2}$ is the standard deviation of A and $\Delta \langle A \rangle = \langle A \rangle - A^*$ the deviation of the mean $\langle A \rangle$ with respect to A^* , one obtains the equivalent definition

Ergodicity condition e1

$$|\Delta \langle A \rangle| \leq \eta_1 \quad (5)$$

Ergodicity condition e2

$$\sigma_A \leq \eta_2.$$

If the conditions in (5) are fulfilled, then the observable A is ergodic within the range $\eta = (\eta_1^2 + \eta_2^2)^{1/2}$. The asymptotic ergodicity in a strict sense, i.e., as discussed by Sposito *et al.* [1986], is ensured when the observable A is the concentration and (5) holds in the large time limit for arbitrary small and positive η_1 and η_2 . In other words, asymptotic ergodicity requires the existence of an upscaled macrodispersion solution for the ensemble averaged concentration, as expressed by condition e1, and a “self-averaging” property, namely the convergence of the actual concentrations to their ensemble average, described by condition e2. When the observable A is a space averaged concentration and the conditions (5) are fulfilled at finite times for increasing dimensions of the averaging domain, then the space averaged concentration converges in the mean square limit to the ensemble averaged concentration and the space and ensemble averages are interchangeable. Condition e2 for space averaged concentration was used by Dagan [1984,

1987] to investigate the ergodicity under the assumption that the ensemble averaged concentration is already Gaussian at finite times. Condition e2 also formulates the self-averaging property of the longitudinal effective coefficient, investigated by *Clincy and Kinzelbach* [2001] and *Eberhard* [2004]. The condition e1 alone, applied to effective coefficients or to second moments of the plume, is often referred to as “ergodicity condition” [*Fiori*, 1998; *Naff et al.*, 1998b; *Zhang and Seo*, 2004; *Dagan*, 2004]. For finite times and ranges η , the definition (5) corresponds to the operational interpretation for ergodicity, proposed by *Kabala and Sposito* [1994], which seeks conditions that lead to acceptably small deviations of the experimentally observable concentrations from the predictions of the stochastic model. The observables A used to quantify the ergodicity in this study are the cross-section space-averaged concentration and the effective diffusion coefficients. The corresponding theoretical predictions A^* are the solutions of the upscaled macrodispersion model.

3. Numerical Approach

3.1. Prerequisites for Numerical Investigations

[22] Numerical investigations on the existence of the diffusion limit and ergodicity require the simulation of large ensembles of realizations of the transport over large traveled distances. Because this task generally surpasses the available computing resources, some compromise was accepted and the efforts focused by now on one or two of the three objectives: (1) accurate concentration field in a given realization, (2) simulations of the transport over large timescales, and (3) reliable statistics for the ensemble of realizations.

[23] For instance, objective 1 was pursued by *Smith and Schwartz* [1980], *Tompson and Gelhar* [1990], *Moltyaner et al.* [1993], *Naff et al.* [1998b], *Kapoor and Kitanidis* [1998], *Trefry et al.* [2003], and *Janković et al.* [2003], where given realizations of the transport were simulated over distances still too small to describe the asymptotic behavior (with the exception of the confined aquifer case considered by *Kapoor and Kitanidis* [1998]). Reliable statistical ensembles (objective 3), aiming to compute the upscaled coefficients (4), were obtained by tracking one particle in 1500 realizations of the velocity field [*Bellin et al.*, 1992], 20 particles in 500 realizations [*Salandin and Fiorotto*, 1998], 20 particles in 1600 realizations [*Zhang and Seo*, 2004], or 10000 particles in 20 realization [*Fernández-García et al.*, 2005a], and averaging over realizations. The computational constraints did not allow the simulation over more than a few of velocity correlation lengths and the asymptotic regime, i.e., constant coefficients \mathbf{D}^* , was not reached.

[24] Objectives 2 and 3 were aimed at by *Schwarze et al.* [2001] and *Dentz et al.* [2002, 2003], in the study of the large time behavior of the effective coefficients in the case of point-like injection. The velocity fluctuations $\epsilon \mathbf{u}$ were numerically approximated using the generator of *Kraichnan* [1970]. The coefficients were computed in two ways: as average over the trajectories of a single particle in thousands of realizations, which corresponds to \mathbf{D}^* in (4), and as average over realizations of the coefficients corresponding to \mathbf{D}^{eff} (2), obtained by tracking a number of particles (between tens and hundreds) released at the same point in each realization. The time

behavior of the two coefficients is different but both tend to the same constant limit, after travel distances of more than 1000 correlations lengths. The numerically simulated limit coefficients were close to the approximations of the order ϵ^2 provided by perturbation analyses.

[25] The objective 1 has not yet been attained at the same time with 2 and 3 due to the limitations of the computational resources. For instance, with regard to the particle tracking method which is the most frequently used in large-scale simulations, it is recognized that the number of particles should be enormous if we want to obtain accurate concentrations in the limit of a few significant figures [*Sun*, 1996, p. 95]. Recent investigations show that convergent simulations for single realizations of the transport problem considered here require a number of particles of the order of tens of billions, which is prohibitive for the particle tracking algorithms [*Vamos et al.*, 2003; *Suciu et al.*, 2004].

[26] Our numerical approach uses the GRW algorithm, a generalized random walk method for which there are no limitations as to the maximum number of particles. *Suciu et al.* [2002, 2004] showed that GRW is appropriate to simulate large-scale transport in groundwater. In this paper we show that GRW fulfils the requirements 1, 2, and 3 from above and makes possible a direct investigation on the ergodicity issue, based on the definition (5).

3.2. Implementation of the GRW Method

[27] We considered two-dimensional divergence-free velocity fields with constant mean $\langle \mathbf{V} \rangle = \mathbf{U} = (U, 0)$, $U = 1$ m/d, given by the Darcy law for normal log hydraulic conductivity y , with isotropic correlation length $\lambda_y = 1$ m, and variance $\sigma_y^2 = 0.1$. They were generated numerically with the Kraichnan procedure which is frequently used in large-scale simulations of transport [*Jaekel and Vereecken*, 1997; *Schwarze et al.*, 2001; *Dentz et al.*, 2002, 2003; *Eberhard*, 2004]. The Kraichnan method ensures the incompressibility and approximates the realizations of the Gaussian velocity field, given by the first-order approximation in σ_y of Darcy and continuity equations, by means of a superposition of sine (or cosine) periodic modes.

[28] In every realization of the velocity field the simulation of an isotropic diffusion ($D_{ll} = D = 0.01$ m²/d, $D_{lm} = 0$ for $l \neq m$) was conducted for dimensionless times Ut/λ_y , corresponding to thousands of correlation lengths, using the reduced fluctuations GRW algorithm presented in section A1. In each realization of the velocity field, $N = 10^{10}$ particles were initially uniformly distributed in a vertical band or located at the origin of the grid. Because the theoretical result presented in section 2.1 was obtained for unbounded domains, the grid was chosen to be larger than the maximum extension of the plume. Implementation details are discussed in section A2. Some preliminary tests have shown that the longitudinal local dispersion has little influence on the resulting concentration fields, in agreement with the results concerning the longitudinal effective coefficients presented by *Fiori* [1996, Figure 1] and by *Dentz et al.* [2000a, Appendix B]. Thus D mainly describes the strength of the transverse local dispersion.

[29] We chose the parameters $\sigma_y^2 = 0.1$ and $D = 0.01$ m²/d after preliminary investigations, presented in section B1. These parameters minimize possible numerical artifacts occurring in two-dimensional simulations using particles methods and Kraichnan generator. The comparison pre-

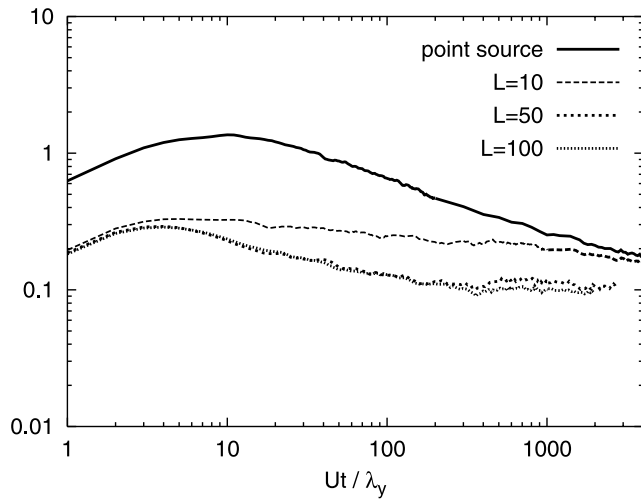


Figure 1. Deviations from the macrodispersion model of the mean concentration at the plume center of mass $\Delta\langle C\rangle/C^*(x_1, t)$.

sented in section B2 shows that the fluctuations have similar large time behavior for exponential and Gaussian shape for the correlation of the log hydraulic conductivity field, provided that the number of periods Np in Kraichnan routine and the number of realizations R are large enough. For the detailed investigations on ergodicity presented in the following we chose the exponential correlation shape, $Np = 6400$ and $R = 256$ realizations. In section B3 it was shown that the numerically generated velocities approximate a Gaussian random field and the squared fluctuations ε^2 have roughly the same order of magnitude as the local dispersion coefficient D (see second row of Table B1), in agreement with the theoretical assumptions leading to an upscaled Gaussian process. The corresponding theoretical values of the longitudinal and transverse effective diffusion coefficients, computed from the first-order estimation of the correlations under the integral in (4) [Dagan, 1984], have the values

$$D_{11}^* = 0.11 \text{ m}^2/\text{day} \quad D_{22}^* = 0.01 \text{ m}^2/\text{d}. \quad (6)$$

[30] The simulations started with a uniform initial distribution of the 10^{10} particles inside rectangles $\lambda_y \times L\lambda_y$, with $L = 10, 50$ and 100 , oriented across the mean flow. In the case of instantaneous point source, all the particles were released from the origin of the grid at the initial time. The total simulation time was of 2000 days for $L = 100$, 2700 days for $L = 50$, and 4000 days for $L = 10$ and for the point source. The cross-section space-averaged concentrations in given realizations $C(x_1, t; L)$ were computed according to (A1) by the number of particles in a domain $\lambda_y \times (160 + L)\lambda_y$ divided by the total number of particles N . The normalized concentrations were obtained through division by the initial concentrations: $C(x_1, t) = C(x_1, t; L)/C(0, 0; L)$. The averaging domain, oriented across the mean flow and centered at x_1 , corresponds to the ideal sampling across reference planes aimed at in field tracer tests [Vanderborght and Vereecken, 2002] as well as in laboratory and numerical experiments [Fernández-García et al., 2005a,

2005b]. We stored the space averaged concentration at the plume center of mass, $C(\langle x_1 \rangle, t)$, as well as the concentration field $C(x_1, t)$ at several fixed times. The effective coefficients (2) were computed according to (A2). Further, we computed the mean concentrations $\langle C \rangle$ and the mean effective coefficients $\langle D_{eff}^* \rangle$, as averages over the ensemble of R realizations of the transport. Since in all the simulations the mean flow velocity was $U = 1$ m/d, the numerical values of the effective coefficients coincide with the dispersivities D^{eff}/U , measured in meters.

4. Numerical Results on Ergodicity

4.1. Cross-Section Averaged Concentrations

[31] Since the width of the averaging domain is larger than the transverse dimension of the plume, the transport can be described by a one-dimensional problem for the spatially averaged concentration $C(x_1, t)$. The corresponding theoretical concentration C^* is the one-dimensional Gaussian distribution of coefficient $D_{11}^* = 0.11 \text{ m}^2/\text{d}$ which describes the cross section average of the concentration predicted by the stochastic macrodispersion model. Ergodicity condition e1 in (5) was investigated by means of the relative deviation of the ensemble average of the cross-section averaged concentration from the theoretical value, $\Delta\langle C\rangle/C^* = (\langle C \rangle - C^*)/C^*$. The deviations $\Delta\langle C\rangle/C^*$, computed at the plume center of mass $\langle x_1 \rangle$ presented in Figure 1 show that in the case of point source at $t = 4000\lambda_y/U$ condition e1 is fulfilled within a range $\eta_1 \simeq 0.17C^*$. The increase of L reduces the deviations at early times. For instance, for $L \geq 50$, $\eta_1 \simeq 0.13C^*$ at 100 advection timescales λ_y/U (or, equivalently at one dispersion timescale λ_y^2/D).

[32] To check the second ergodicity condition e2 we used the standard deviation of the cross-section averaged concentration divided by the theoretical solution σ_C/C^* , where $\sigma_C = (\langle C^2 \rangle - \langle C \rangle^2)^{1/2}$. The results presented in Figure 2 show that for point source at $t = 4000\lambda_y/U$, condition e2 is fulfilled within a range $\eta_2 \simeq 0.11C^*$. Thus, according to (5) the ergodicity range is $\eta = (\eta_1^2 + \eta_2^2)^{1/2} \simeq 0.2C^*$. The monotonous decay of the mean square deviation

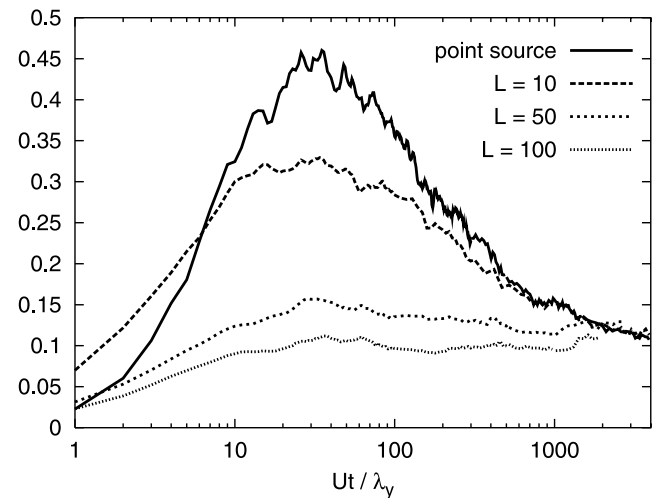


Figure 2. Standard deviations of the concentration at plume center of mass $\sigma_C/C^*(\langle x_1 \rangle, t)$.

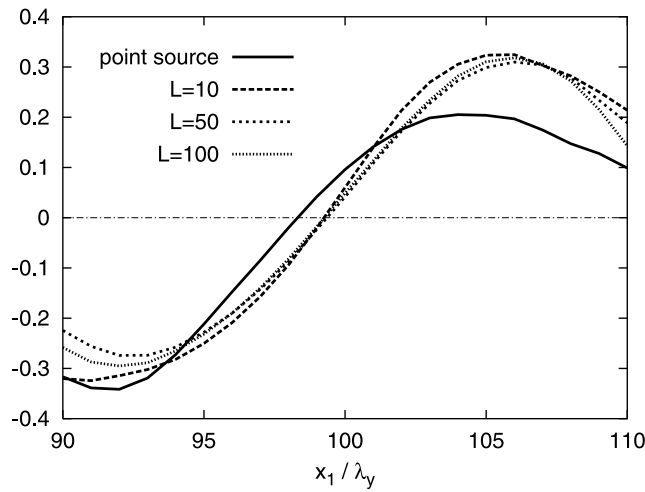


Figure 3. Deviations from the macrodispersion model of the mean concentration as space function $\Delta\langle C \rangle / C^*(x_1, 100\lambda_y/U)$.

$(\Delta C)^2 = \sigma_C^2 + (\langle \Delta C \rangle)^2$ indicate the convergence in mean square limit of the cross-section averaged concentration to the solution of the macrodispersion process.

[33] For $L = 100$ at one dispersion timescale one obtains in a similar way $\eta_2 \simeq 0.1C^*$ and $\eta \simeq 0.16C^*$. The results for ensemble averaged concentration as function of the distance from the center of the initial plume for a fixed time of $100\lambda_y/U$, presented in Figures 3 and 4, indicate that η has a minimum at $x_1 = 100\lambda_y$ (which corresponds to the mean center of mass coordinate). A rough prediction of the maximum concentration estimated by the cross-section averaged concentration at the plume center of mass, $C^* \pm 3\eta$, is reliable for almost all the realizations of the ensemble defined by a given statistical structure of the log hydraulic conductivity. In the somewhat ideal case analyzed here, for initial plumes extending over 100 correlation lengths across the mean flow, the prediction based on the macrodispersion model and the ergodic hypothesis of the space averaged concentration C in actual aquifers is affected by uncertainties of the order $6\eta \simeq 0.9C^*$.

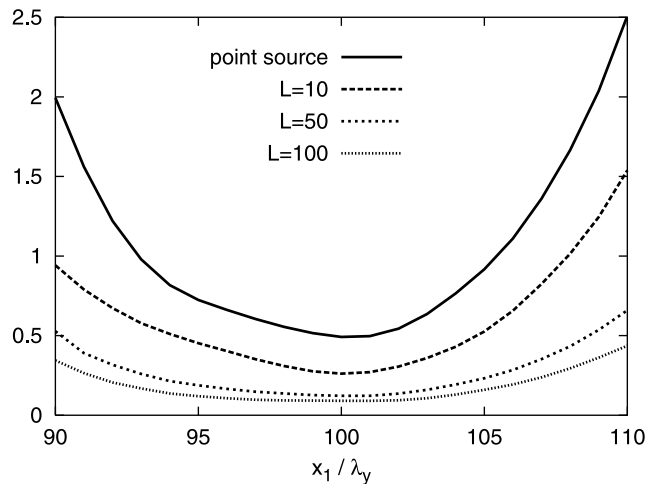


Figure 4. Standard deviations of the concentration as space function $\sigma_C / C^*(x_1, 100\lambda_y/U)$.

[34] The behavior of standard deviations presented in Figure 2 indicate a nonlinear dependence on the plume dimension at early times. For large sources ($L \geq 50$) the concentration fluctuations σ_C / C^* are smaller than in the case of point source, decrease with L and remain almost constant, at values about 0.1, over more than thousand advection timescales. The monotonous decrease of the fluctuations, i.e., the asymptotic ergodicity, does not occur until the end of the simulations.

4.2. Effective Coefficients

[35] The relative deviation of the ensemble averaged effective coefficients from the theoretical values given in (6) can be expressed using (3) by

$$\begin{aligned} \Delta\langle D_{ll}^{eff} \rangle / D_{ll}^* &= (\langle D_{ll}^{eff} \rangle - D_{ll}^*) / D_{ll}^* \\ &= \Delta\langle \tilde{D}_{ll} \rangle / D_{ll}^* + \sigma_{0,ll}^2 / (2tD_{ll}^*). \end{aligned} \quad (7)$$

Since the contribution of the initial plume $\sigma_{0,ll}^2 / (2tD_{ll}^*)$ is a deterministic quantity which tends to zero for large times, to compare the asymptotic behavior of the effective coefficients for different L we used the deviation of the mean slope of the second centered moment of the plume $\Delta\langle \tilde{D}_{ll} \rangle / D_{ll}^*$. The results for longitudinal coefficients are presented in Figure 5. Ergodicity condition e1 for the mean slope is fulfilled within a range $\eta_1 \simeq 0.11D_{11}^*$ in the case of point source at 4000 advection times and within a range $\eta_1 \simeq 0.05D_{11}^*$ in the case $L = 100$ at 100 advection times. Because $\sigma_{0,11}^2 = 0.1 \text{ m}^2$ in all cases, at $t = 100\lambda_y/U$ its contribution in (7) is already only 0.0045 and therefore the same range η_1 characterizes the longitudinal effective dispersion coefficients.

[36] Because \tilde{D}_{ll} and D_{ll}^{eff} differ by a deterministic quantity, as shown by (3), they have the same fluctuations. The fluctuations $\sigma_{D_{11}^{eff}} / D_{11}^*$ of the longitudinal effective dispersion coefficient are given in Figure 6. For a small increase of the plume dimension, the fluctuations increase (similarly to the results reported by Naff *et al.* [1998b, Figure 15]) and they decrease when the plume dimension is further increased, like the fluctuations of the cross-section averaged

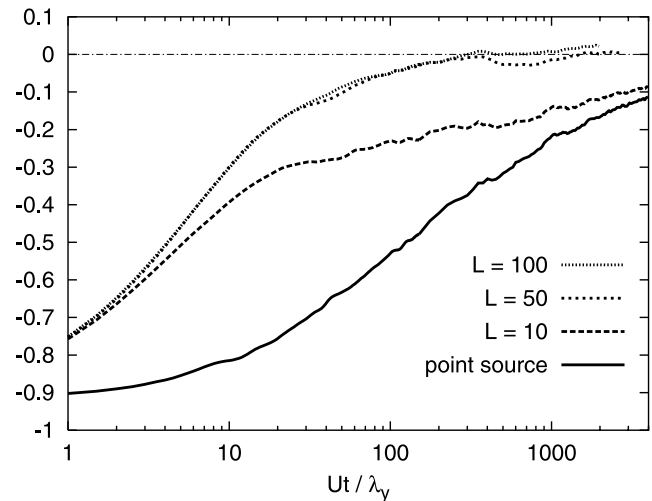


Figure 5. Deviations from the macrodispersion model of the mean slope of the longitudinal second moment $\Delta\langle \tilde{D}_{11} \rangle / D_{11}^*$.

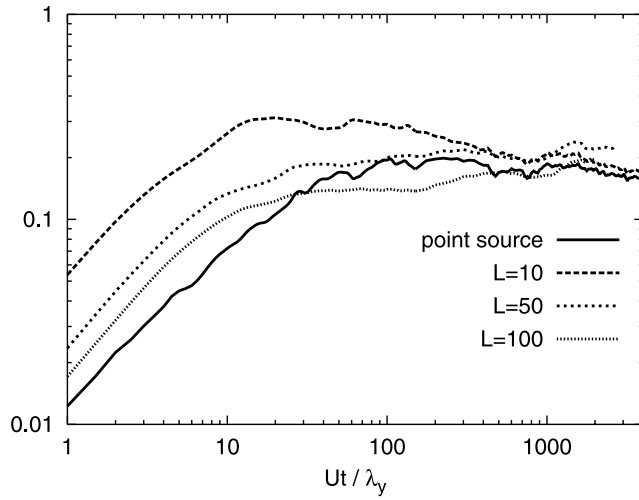


Figure 6. Fluctuations of the longitudinal effective dispersion coefficient $\sigma_{D_{11}^{eff}}/D_{11}^*$.

concentration in Figure 2. Ergodicity condition e2 is fulfilled within a range $\eta_2 \simeq 0.16 D_{11}^*$ for point source at $t = 4000 \lambda_y/U$ and within a range $\eta_2 \simeq 0.14 D_{11}^*$ in the case $L = 100$ at $t = 100 \lambda_y/U$. It follows that, according to (5), the corresponding ergodicity ranges are $\eta \simeq 0.2 D_{11}^*$ (point source) and $\eta \simeq 0.15 D_{11}^*$ ($L = 100$). The large time behavior for small sources ($L \leq 10$), shown in Figures 5 and 6, indicates the asymptotic ergodicity of the longitudinal effective coefficient. The deviations from the macrodispersion model of the mean slope of the transverse second moment and the fluctuations of the transverse effective coefficients, presented in Figures 7 and 8, respectively, show that the transverse mean slope coefficient \tilde{D}_{22} behaves asymptotically ergodic. Since $\sigma_{\tilde{D}_{22}}^2/(2tD_{22}^*)$ goes to zero at large times, from (7) and Figure 7 it follows that the effective transverse coefficient is also asymptotically ergodic.

[37] The asymptotic effective coefficients and their deviation from the theoretical values D_{ii}^* were computed in the case $L = 100$ as follows. First, the temporal averages of the

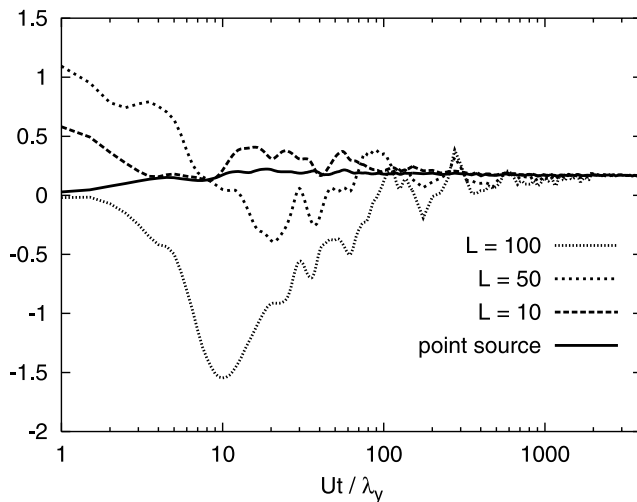


Figure 7. Deviations from the macrodispersion model of the mean slope of the transverse second moment $\Delta\langle\tilde{D}_{22}\rangle/D_{22}^*$.

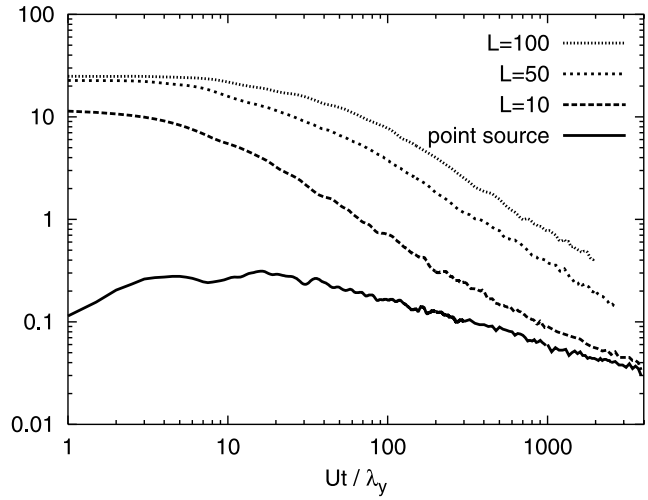


Figure 8. Fluctuations of the transverse effective dispersion coefficient $\sigma_{D_{22}^{eff}}/D_{22}^*$.

mean slopes \tilde{D}_{ii} between $t = 200 \lambda_y/U$ and $t = 2000 \lambda_y/U$, $[\tilde{D}_{ii}]$, were computed in every realization. Then, averages over realizations were used to estimate the mean asymptotic coefficients $D_{ii}^\infty = \langle[\tilde{D}_{ii}] \rangle$ and the deviations

$$\Delta[\tilde{D}_{ii}] = \left(\langle ([\tilde{D}_{ii}] - D_{ii}^*)^2 \rangle \right)^{1/2}$$

with respect to D_{ii}^* . The results are presented in Figure 9 as functions of the number of realizations R . The fact that the deviations of the mean coefficients D_{ii}^∞ from D_{ii}^* are one order of magnitude smaller than the local dispersion coefficient D , in very good agreement with (4), constitutes a test for the accuracy of the numerical simulations. The behavior of the deviations $\Delta[\tilde{D}_{ii}]$ (thin lines in Figure 9) indicate that the time averaged coefficients $[\tilde{D}_{ii}]$ are ergodic within a range of the order of the local dispersion coefficient $\eta \simeq D = 0.01 \text{ m}^2/\text{d}$.

[38] Even if the mean slope is ergodic within an acceptable small range, the macrodispersion coefficients D_{ii}^*

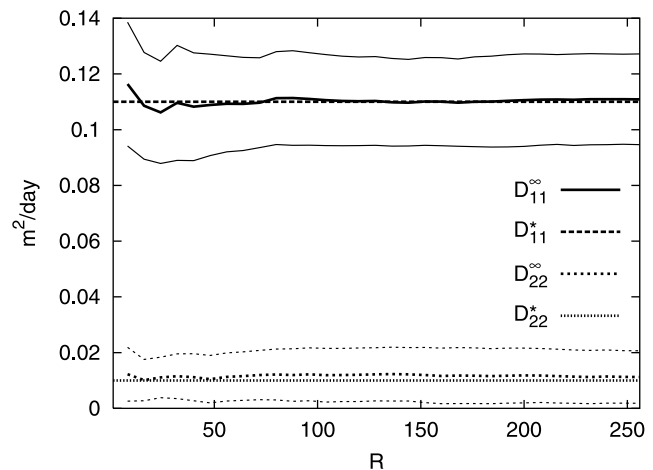


Figure 9. Asymptotic effective coefficients and deviations from the theoretical values (6) for $L = 100$, as functions of the number of realizations R .

describe the time behavior of the second moments of the plume with errors smaller than 100% only when, according to (7), $\sigma_{0,II}^2/(2tD_{II}^*) \leq 1$. For the transverse coefficient the corresponding time $\sigma_{0,22}^2/(2D)$ can be very large (tens of thousands of advection scales for $L \geq 50$) and increases proportionally with L^2 . Figures 2, 6, and 8 indicate that the fluctuations are also characterized by time scales which increase with the plume dimension L . This finding agrees with the exact analytical result of *Clincy and Kinzelbach* [2001]. Figure 4 in their paper shows that the fluctuations of the longitudinal coefficient tend to an asymptotic value (which is finite in the case of the model of G. Matheron and G. de Marsily studied there) after times of the order of L^2/D , i.e., the time for a dispersive spreading of the solute over the width L of the initial plume. On this timescale the transport becomes independent of the extent and shape of the initial plume. This is also indicated by the behavior of the cross-section concentrations (Figures 1 and 2) and of the mean slope coefficients (Figures 5–8) for $L = 10$ and point source, which after 4000 advection times reach almost the same ergodicity range η . Similar time behavior was found by *Dentz et al.* [2000b, Figure 1] for the ensemble averaged longitudinal dispersion coefficient of extended plumes (defined as half the derivative of the second moment). The total time in our simulations is still too small to allow an estimation of the asymptotic ergodicity timescale. However, the numerical findings and the two theoretical results mentioned above indicate that the ergodicity scale increases like L^2 .

4.3. Time Behavior of the Effective Coefficients and Ergodicity

[39] As shown by equation (A3) in section A1, the GRW procedure computes the variance of displacements \mathbf{X} in a single realization as an average over the realizations of the local dispersion process and over the distribution of the particles inside the initial plume. The ensemble average of the variance can be written as

$$\begin{aligned} \langle \sigma_{II}^2 \rangle_V &= \langle \langle X_I^2 \rangle_{D,X_0} - \langle X_I \rangle_{D,X_0}^2 \rangle_V \\ &= \left(\langle X_I^2 \rangle_{D,X_0,V} - \langle X_I \rangle_{D,X_0,V}^2 \right) - \left(\langle \langle X_I \rangle_{D,X_0}^2 \rangle_V - \langle X_I \rangle_{D,X_0,V}^2 \right), \end{aligned} \quad (8)$$

where the subscripts D , X_0 and V denote the average over the realizations of the local dispersion, the initial distribution of the particles, and the realizations of the random velocity field respectively. This obvious relation shows that $\langle \sigma_{II}^2 \rangle_V$ is the difference between the variance with respect to the ensemble average of the center of mass $R_I = \langle X_I \rangle_{D,X_0}$ and the variance of the center of mass $R_{II} = \langle R_I^2 \rangle_V - \langle R_I \rangle_V^2$. Assuming that the averages over initial positions and velocity realizations have the following permutation property $\langle \cdots \rangle_{D,X_0,V} = \langle \cdots \rangle_{D,V,X_0}$, the first term in (8) becomes

$$\langle \langle X_I^2 \rangle_{D,V} - \langle X_I \rangle_{D,V}^2 \rangle_{X_0} + \langle \langle X_I \rangle_{D,V}^2 \rangle_{X_0} - \langle X_I \rangle_{D,X_0,V}^2.$$

For statistical homogeneous velocity fields it seems reasonable to assume the independence of the averages $\langle \tilde{X}_I \rangle_{D,V}$ and $\langle \tilde{X}_I^2 \rangle_{D,V}$ where $\tilde{X}_I = X_I - X_0$, from the initial state \mathbf{X}_0 . Then, the last two terms above give the initial variance $\sigma_{0,II}^2 = \langle X_{0I}^2 \rangle_{X_0} - \langle X_{0I} \rangle_{X_0}^2$ and the first term becomes

independent of \mathbf{X}_0 and represents the variance around the ensemble averaged center of mass for the process starting with a point-like injection at $\tilde{X}_I = 0$, $\tilde{X}_{II} = \langle \tilde{X}_I^2 \rangle_{D,V} - \langle \tilde{X}_I \rangle_{D,V}^2$. Finally, the ensemble average (8) of the second centered moment of the plume becomes

$$\langle \sigma_{II}^2 \rangle_V = \sigma_{0,II}^2 + \tilde{X}_{II} - R_{II}. \quad (9)$$

The variance \tilde{X}_{II} is just the II component of “the second spatial covariance of an ergodic plume” frequently used in investigations on ergodicity [Zhang and Lin, 1998; Zhang and Seo, 2004]. When the local dispersion is neglected, (9) is identical to relation (11) of *Dagan* [1990], derived in the hypothesis of “Lagrangian stationarity” and using the permutation of averages over initial states and velocity realizations. The explicit dependence of \tilde{X}_{II} on local dispersion and velocity correlations can be derived from descriptions of the transport process in terms of trajectories [Rajaram and Gelhar, 1993a; Fiori, 1998] or by using the advection-dispersion equation [Kitanidis, 1988; Rajaram and Gelhar, 1993b].

[40] Dividing both sides of (9) by $2t$ and using (2), the ensemble averaged effective coefficients can be written as

$$\langle D_{II}^{eff} \rangle_V(t) - \frac{\sigma_{X_{0,II}}^2}{2t} = D_{II}^{erg}(t) - D_{II}^{cm}(t). \quad (10)$$

The “center of mass coefficient” $D_{II}^{cm} = R_{II}/(2t)$ corresponds to the “pseudodispersivity” investigated numerically by *Naff et al.* [1998b]. The first term in the right side of (10), $D_{II}^{erg} = \tilde{X}_{II}/(2t)$ is the so-called “ergodic coefficient” which is expected to become constant and equal to the upscaled macrodispersion coefficient in the large time limit [Dagan, 1990]. The condition $D_{II}^{cm} = 0$ is referred to as “ergodicity condition” [Fiori, 1998; Naff et al., 1998b; Zhang and Seo, 2004; Dagan, 2004]. The ergodic coefficients correspond to the “ensemble coefficients” introduced by *Attinger et al.* [1999] (where the ensemble and effective coefficients are defined by the time derivative of the corresponding variances related by (8)). Under the assumption of statistical homogeneity of the log hydraulic conductivity the ensemble coefficients were also shown to be independent of the shape and dimension of the initial plume and equal to the coefficients for the case of a point source [Dentz et al., 2000b; Clincy and Kinzelbach, 2001]. Zhang and Seo [2004] have shown that, even for statistically anisotropic aquifers, the longitudinal and transverse ergodic second moments given by theory can be retrieved in numerical simulations by using the relation (9). However, analyzing the fluctuations of the longitudinal effective coefficient from realization to realization, *Naff et al.* [1998b] found a “nonergodic behavior,” indicated by the increase of the fluctuations with the transverse dimension of the plume, and suggested that the approach to a quasi-ergodic state is more complicated than described by the equation (10). In the following we investigate this issue in the light of our GRW simulations.

[41] The longitudinal center of mass coefficient decreases with the plume dimension (Figure 10) and the ergodic coefficient derived from (10) is practically independent of the plume dimensions (Figure 11). This agrees with the results for the ergodic second moments of the plume

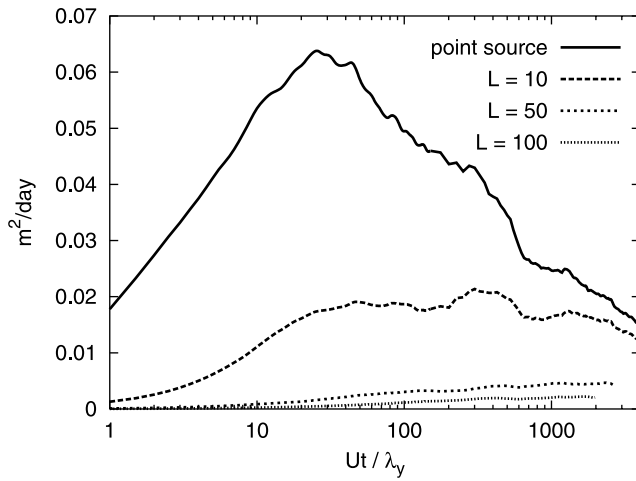


Figure 10. Time behavior of the longitudinal center of mass coefficient D_{11}^{cm} .

obtained by *Zhang and Lin* [1998, Figure 9] and *Zhang and Seo* [2004, Figure 5] and the results for the longitudinal center of mass coefficient of *Naff et al.* [1998b, Figure 14]. D_{11}^{cm} is the difference between the ergodic coefficient D_{11}^{erg} and the ensemble average of the mean slope (3), $\langle \tilde{D}_{11} \rangle_v$, given by the left side of (10). A small center of mass coefficient $D_{11}^{cm}(t) \leq \eta_1$ is equivalent to ergodicity condition e1 in (5), for the deviation of the ensemble average of the observable $A(t) = \tilde{D}_{11}(t)$ from the theoretical prediction $A^*(t) = D_{11}^{erg}(t)$. The increase of fluctuations with the plume dimension reported by *Naff et al.* [1998b, Figure 15] simply means that the vanishing center of mass coefficients in (10) is not sufficient to ensure the ergodicity of the mean slope of the second moment of the plume. Even though the center of mass coefficients become negligible quantities and the ensemble averaged slope approach the ergodic coefficient, the sample-to-sample fluctuations can be still large. This situation is dramatically illustrated in the case of the transverse coefficients. After 1000 advection times the first ergodicity condition e1 is fulfilled within a range two orders of magnitude smaller than the local dispersion coefficient, as shown by the behavior of D_{22}^{cm} in Figure 12. The

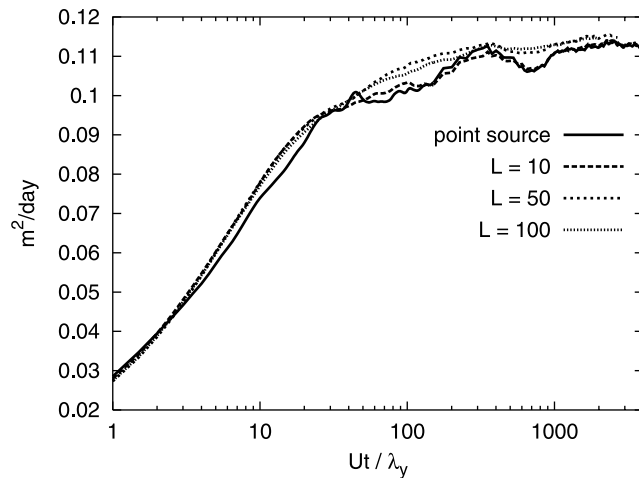


Figure 11. Time behavior of the longitudinal ergodic coefficient D_{11}^{erg} .

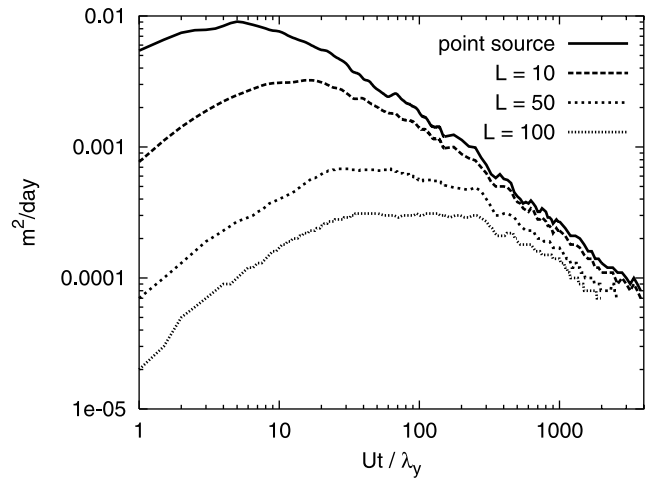


Figure 12. Time behavior of the transverse center of mass coefficient D_{22}^{cm} .

fluctuations of the mean slope \tilde{D}_{22} , which are equal to the fluctuations of the effective coefficients in Figure 8, indicate that the second condition e2 is not fulfilled within the same range. Moreover, the larger the transverse dimension of the plume is, the less ergodic the transverse coefficients are.

[42] We comment here that the coefficient corresponding to $L = 100$ in Figure 13 has negative values at early times. This nonphysical behavior occurs because in the left side of (10) the contribution of the initial plume was extracted from the total variance. This “bad result” shows that the definition of the effective coefficients by the mean slope of the variance fails to describe the plume at finite times. We also note that the negative effective transverse dispersivities obtained, in three-dimensional case, by *Zhang et al.* [1996] are due to their definition by the local slope of the second moment, and are not “an artifact of the first-order approximation,” as the authors suggest. It is indeed easy to see that there are no negative values if the dispersivities are computed by using the positive-definite coefficient (2) and the variances shown in Figure 2b of the quoted paper. The same explanation is valid for the negative dispersivities

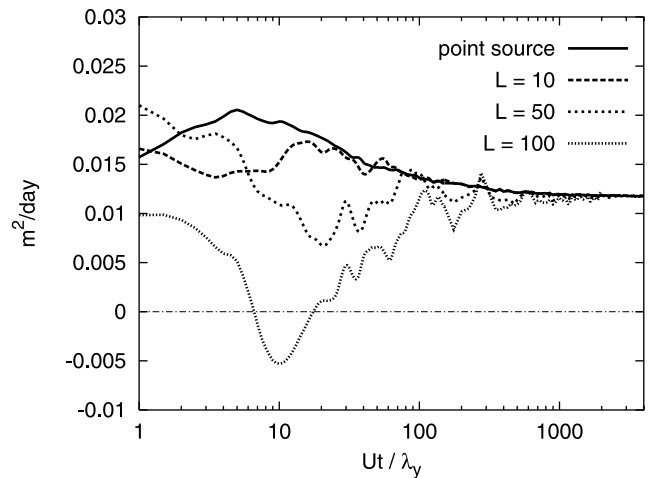


Figure 13. Time behavior of the transverse ergodic coefficient D_{22}^{erg} .

obtained for two-dimensional plumes by first-order theoretical analysis [Zhang and Zhang, 1997, Figure 2e] and numerical simulations [Zhang and Lin, 1998, Figure 10].

[43] The large differences between the coefficient for point source and the coefficients for $L \geq 10$ shown in Figure 13 prove that for plumes with large transverse dimensions the ergodic coefficient for preasymptotic regime cannot be defined by (10). Unlike the center of mass coefficients (Figure 12) which go to zero, the differences between the ergodic coefficients increase with the plume dimension. These deviations can be neglected only for small plumes, as indicated by the three-dimensional simulations for $L \leq 4$ of Zhang and Seo [2004, Figures 5b and 5c] and by the two-dimensional simulations for $L \leq 10$ of Zhang and Lin [1998, Figure 9]. (Note that the small differences reported in these papers are also due to the graphical representation based on relation (9); this representation also reduces the differences shown in our Figure 13.) This dependence on the plume dimension could be a consequence of the inherent nonhomogeneity of the numerically generated velocity field. However, in practice, the statistical homogeneity is always an approximation. This is shown, for instance, by the behavior of the confidence intervals rendered by the uncertainty of the statistical parameter estimates in carefully designed laboratory experiments [Fernández-García et al., 2005b], which are very similar to those for the numerical velocity field presented in Figure B7. However, even if the lack of strict statistical homogeneity can produce the small differences for the longitudinal coefficients in Figure 11, it does not explain the large differences shown in Figure 13. Therefore the very validity of the relation (10) can be questioned.

[44] The assumption that the average over initial positions permutes with the average over the realizations of the velocity field, on which (10) is based, is not always true. For instance, when local dispersion is neglected and the transport process is described in a Lagrangian framework, the above permutation of averages is allowed by the “simplifying assumption of ergodicity in the plume spatial moments” [Sposito and Dagan, 1994, p. 588] (carrying the implicit hypothesis of “dynamically identical” solute particles described by a single statistical ensemble [Sposito, 1997]). It was already shown by Sposito and Dagan [1994] that in the purely advective case the relation (10) is not complete if the interdependence between the initial positions and the velocities of the solute particles is taken into account. Because for Darcy flows such interdependencies cannot be ignored (unless some restrictions on the flow domain are imposed) [Sposito, 1997, 2001], it follows that in general this relation is not true. Since the dynamical system approach used in the papers quoted above is restricted to the advective case, the analysis of the relation (10) in the case of nonvanishing local dispersion calls for further investigations based on appropriate methods.

5. Conclusions

[45] The results obtained in the present study, indicate that the numerical approach was appropriate for a numerical investigation on the ergodicity of transport in heterogeneous aquifers. The requirements of accurate concentration in every realization of the random field, long time simulations

of transport and large statistical ensembles of realizations were carried out with the GRW algorithm. The large-scale simulations were also possible owing to the fast generator of the first order approximated Darcy velocity fields, based on the Kraichnan routine. The approximation of the Gaussian random velocity fields with periodic fields was shown to be reliable for 6400 modes in the Kraichnan algorithm. The quantitative assessment of ergodicity for space averaged concentrations and effective diffusion coefficients was done via comparisons with a rigorous mathematical result on the existence of the upscaled macrodispersion process which describes the ensemble averaged concentration asymptotically. We emphasize that the conclusions drawn below are valid for small heterogeneity of the aquifer, which allows comparisons with the mathematical result, and cannot be simply extrapolated for highly heterogeneous formations.

[46] A numerical evidence for the asymptotic ergodic behavior of the two-dimensional transport was supplied by the simulations in the case of point-like and small initial plumes. The time to reach acceptably small deviations from the predictions of the macrodispersion model is of thousands of advection timescales. In rapidly fluctuating velocity fields with advection times of the order of seconds, for instance in the case of turbulent transport in atmosphere, the ergodic behavior manifests after a few hours. Since the advection times in groundwater are of the order of days, the ergodic behavior in a strict sense can be expected when the plume has traveled tens of years. This could be useful in applications for persistent contaminants, like the long life radionuclides.

[47] For sufficiently large initial plumes, the macrodispersion model can be used to predict the contamination with errors that could be acceptable in forecasting at smaller timescales. For instance, when the initial plume extends over one hundred heterogeneity scales across the direction of the mean flow, and the solute plume has traveled hundreds of heterogeneity scales, the “three sigma” rule indicates that the cross-section averaged concentration and the longitudinal effective coefficient in given realizations can be predicted within a range of uncertainty of about 90%. This uncertainty remains almost constant over thousands of heterogeneity scales. In the same conditions, the uncertainty of the transverse coefficient is tens of times larger.

[48] Nevertheless, the common belief that large plumes have ergodic behavior should be amended. The fluctuations from realization to realization have an intricate nonlinear dependence on the transverse dimension of the initial plume, for both cross-section space averaged concentrations and effective diffusion coefficients. For concentration and longitudinal effective coefficient, the fluctuations decrease when the transverse plume dimension is larger than ten correlation lengths, but the traveltime to reach the monotonous decay toward a quasi-ergodic state is much larger than for small sources. For the transverse effective coefficient the fluctuations increase with the dimension of the initial plume at all times. It is expected that the timescale which characterizes the ergodicity increases like the square of the transverse dimension of the initial plume.

[49] The evolution of the ensemble averaged effective coefficients also shows features not accounted for by the existing theory. The slope of the displacements variance,

often used to estimate the effective coefficients, yields nonphysical (negative) estimations of the transverse coefficients at tens of advection timescales. Therefore the rate of increase of the variance, which describes the spatial extension of the plume and is positive-definite, is the appropriate definition for the effective coefficients. The condition of vanishing center of mass coefficient in the large time limit was also found to be not sufficient for the assessment of the ergodic behavior. The failure of the usual approach to define a transverse “ergodic coefficient” for extended initial plumes indicates a dependence on initial conditions, similar to the purely advective case, which deserves further investigations.

Appendix A: Global Random Walk

A1. Algorithm

[50] The GRW algorithm is a generalization of particle tracking method which increases the speed of the computations and considerably improves the accuracy of the numerical simulations [Vamoş *et al.*, 2003]. The solution of a parabolic equation of form (1) is described using N particles which move in a grid, undergoing advective displacements and diffusive jumps according to the random walk law. The concentration field at a given time $t = k\delta t$ and at a grid point $(x_1, x_2) = (i_1\delta x_1, i_2\delta x_2)$ is given by

$$c(x_1, x_2, t) = \frac{1}{N\Delta_1\Delta_2} \sum_{i'_1=-s_1}^{s_1} \sum_{i'_2=-s_2}^{s_2} n(i_1 + i'_1, i_2 + i'_2, k), \quad (\text{A1})$$

where $\Delta_l = 2s_l\delta x_l$, $l = 1, 2$, are the lengths of the symmetrical intervals centered at x_l and $n(i_1, i_2, k)$ is the number of particles which at time step k lie at the grid point (i_1, i_2) .

[51] The one-dimensional GRW algorithm describes the scattering of the $n(i, k)$ particles from (x_i, t_k) by

$$n(j, k) = \delta n(j, j + v_j, k) + \delta n(j + v_j - d, j, k) + \delta n(j + v_j + d, j, k),$$

where v_j are discrete displacements in a given velocity field and d describes the diffusive jumps. The quantities δn are Bernoulli random variables and describe respectively, the number of particles which remain at the same grid site after an advective displacement, the number of particles jumping to the left and those jumping to the right (with respect to the advected position). The distribution of the particles at the next time $(k + 1)\delta t$ is given by

$$n(i, k + 1) = \sum_j \delta n(i, j, k).$$

The average number of particles undergoing diffusive jumps and the average number of particles remaining at the same node after the displacement v_j are given by the relations

$$\overline{\delta n(j + v_j \pm d, j, k)} = \frac{1}{2} r \overline{n(j, k)},$$

$$\overline{\delta n(j, j + v_j, k)} = (1 - r) \overline{n(j, k)},$$

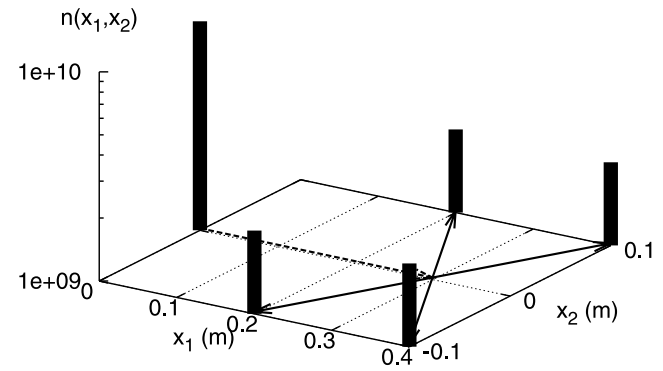


Figure A1. Advective displacement and diffusive jumps of 10^{10} particles starting at $(0, 0)$ for $d = 1$ and $r = 1$.

where $0 \leq r \leq 1$. The diffusion coefficient D is related to the grid steps by the relation

$$D = r \frac{(d\delta x)^2}{2\delta t}.$$

For two and three-dimensional cases, the same procedure is repeated for all space directions.

[52] Because the total number of particles N contained in the grid is conserved, the GRW algorithm is stable. The condition $r \leq 1$, ensures that there is no numerical diffusion. Vamoş *et al.* [2003] showed that for Gaussian diffusion the numerical solution converges as $\mathcal{O}(\delta x^2) + \mathcal{O}(N^{-1/2})$, i.e., for large numbers of particles the convergence order is $\mathcal{O}(\delta x^2)$, the same as for the finite differences scheme. A comparison with a particle tracking code (diffusion over ten time steps of N particle starting at the center of a cubic grid) shows that while in GRW algorithm there is practical no limitation, $N > 10^9$ particles becomes prohibitive for the particle tracking method.

[53] The “reduced fluctuations” GRW algorithm is defined by

$$\delta n(j + v_j - d, j, k) = \begin{cases} n/2 & \text{if } n \text{ is even} \\ [n/2] + \theta & \text{if } n \text{ is odd} \end{cases},$$

where $n = n(j, k) - \delta n(j, j + v_j, k)$, $[n/2]$ is the integer part of $n/2$ and θ is a variable taking the values 0 and 1 with probability 1/2. This algorithm is appropriate for large-scale problems, for two reasons. Firstly, the diffusion front does not extend beyond the limit concentration defined by one particle at a grid point, keeping a physical significant shape (unlike in finite differences where a pure diffusion front has a cubic shape of side $\sim (2Dt)^{1/2}$). Second, the “reduced fluctuations” algorithm requires only a minimum number of calls of the random number generator. Figure A1 illustrates the reduced fluctuations GRW algorithm for $r = 1$, and Figure A2 presents the resulting concentration field computed by (A1).

[54] In the following we describe the computation of the diagonal effective coefficients, according to the GRW algorithm. The variance of particles displacements, σ_{il}^2 , $l = 1, 2$, in dimensionless form, is given by

$$\frac{1}{(\delta x)^2} \sigma_{il}^2(k\delta t) = \frac{1}{N} \sum_{i_1, i_2} i_l^2 n(i_1, i_2, k) - \left[\frac{1}{N} \sum_{i_1, i_2} i_l n(i_1, i_2, k) \right]^2. \quad (\text{A2})$$

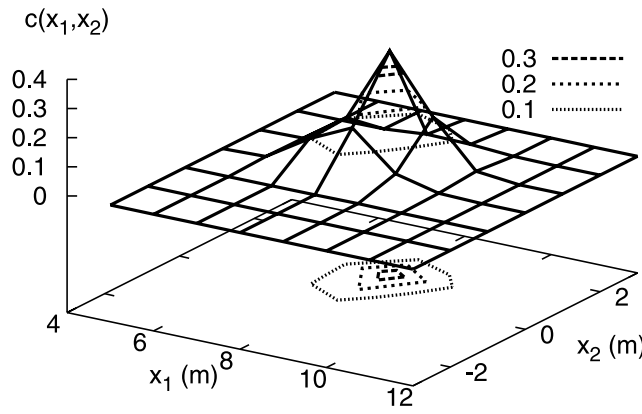


Figure A2. Concentration field, according to (A1), at $t = 10\delta t$, for $\delta x_1 = \delta x_2 = 0.1$ m and $\Delta_{x_1} = \Delta_{x_2} = 1$ m.

Using (A2), the effective coefficients are computed as

$$D_{ll}^{eff}(k\delta t) = \sigma_{ll}^2 / (2k\delta t).$$

[55] Let us consider N_{x_0} points uniformly distributed inside the initial plume, N/N_{x_0} particles at each initial point and let $n(i_1, i_2, k; i_{01}, i_{02})$ be the distribution of particles at the time step k given by the GRW procedure for a diffusion process starting at $(i_{01}\delta x_1, i_{02}\delta x_2)$. Writing the distribution for the extended plume as

$$n(i_1, i_2, k) = \sum_{i_{01}, i_{02}} n(i_1, i_2, k; i_{01}, i_{02}),$$

the averages from (A2) can be rewritten in the form

$$\frac{1}{N} \sum_{i_1, i_2} \alpha n(i_1, i_2, k) = \frac{1}{N_{x_0}} \sum_{i_{01}, i_{02}} \left(\frac{N_{x_0}}{N} \sum_{i_1, i_2} \alpha n(i_1, i_2, k; i_{01}, i_{02}) \right), \quad (A3)$$

where α stands for i_l and i_l^2 respectively. It follows from (A3) that the variance (A2) is an average over the trajectories of the diffusion process starting at given initial positions and over the distribution of the initial positions.

A2. GRW Parameters

[56] The large-scale computations reported by *Schwarze et al.* [2001] and *Dentz et al.* [2002, 2003] were performed with the particle tracking procedure. Although it was possible to obtain estimations of the ensemble averaged effective coefficients, the number of particles used in these simulations, limited due to computational reasons at $N \sim 100$, does not suffice to simulate accurate concentrations. Even in small-scale one-dimensional problems, more than one million particles should be used in particles methods to reach the same precision as the finite difference scheme [*Vamoş et al.*, 2003]. Moreover, *Suciu et al.* [2004] showed that for the large scale transport problem considered here, a too small number of particles induces large numerical errors in the simulation of the time behavior of the effective coefficients. The statistical convergence of the simulations for a given realization of the velocity is ensured only when billions of particles are used. In the present numerical

investigations the number of particles was fixed at $N = 10^{10}$ so that all the simulations of transport realizations were statistically convergent.

[57] The other GRW parameters used for the computation of the ensembles of realizations presented in this paper are the space steps $\delta x_1 = \delta x_2 = \delta x = 0.1$ m, the time step $\delta t = 0.5$ days and the amplitude of the diffusive jumps (see section A1) $d = 2$. The accuracy of the numerical velocity field is governed by the ratio of the log-hydraulic conductivity correlation length to the space step. In our case, $\lambda_y/\delta x = 10$ and fulfils the condition $\lambda_y/\delta x \geq 4$, generally recommended in literature [*Ababou et al.*, 1989; *Hassan et al.*, 1998]. To reduce the “overshooting” errors in particles methods one imposes that the mean displacement in a time step does not surpass a given threshold [*Roth and Hammel*, 1996; *Janković et al.*, 2003]. *Suciu et al.* [2004] showed that for the same overshooting, the error in GRW simulations is mainly influenced by the discretization of the velocity, as described by the parameter $U\delta t/\delta x$. Our choice $U\delta t/\delta x = 5$ means that, in average, the particles overpass 5 space steps, but it also means that the smallest advective displacement accounted for in the GRW procedure is $\delta x/\delta t = U/5 = 0.2$ m/d. The tests for a crude estimation of the discretization errors, for fixed $\delta t = 0.5$ day and increasing $U\delta t/\delta x$ from 5 to 10 ($\delta x/\delta t$ from 0.2 m/d to 0.1 m/d), show that the simulated effective coefficients differ with less than 2% (N. Suciu et al., Numerical investigations on ergodicity of solute transport in heterogeneous aquifers, Internal Report ICG-IV 00204, Forschungszentrum Jülich, 2004). A comparison for the first 100 days with a GRW algorithm without overshooting led to error estimations for the effective coefficients in given realizations, calculated with the GRW procedure and the parameters used in this paper, which were one order of magnitude smaller than the upscaled coefficients (6) [*Suciu et al.*, 2005].

Appendix B: Large-Scale Simulations

B1. Transport Problem

[58] The transport depends on both the heterogeneity of the advection velocity field, described by the variance of the log hydraulic conductivity σ_y^2 , and the local dispersion coefficient D . To select the parameters to be used in the present numerical investigations, several combinations of σ_y^2 and D were investigated in the case of point source (N. Suciu et al., Internal Report ICG-IV 00204, Forschungszentrum Jülich, 2004). The diffusion fronts, defined by grid points containing at least one particle, are compared in Figure B1. We note that large variances of the log hydraulic conductivity ($\sigma_y^2 = 1$) yield non-Gaussian asymmetric plumes.

[59] It should be noted that the asymmetry of the diffusion fronts can be due to a numerical artifact occurring in two-dimensional simulations based on particles methods and Kraichnan fields. In the absence of the third component of the velocity, the probability of occurrence of very small or null advection displacements is high enough to delay some particles with respect to the plume center of mass. This effect is compensated by diffusive displacements, when the local dispersion is large enough [*Suciu et al.*, 2002]. At the limit of zero local dispersion, trapping zones occur causing the fragmentation of the plume and the linear increase of the effective coefficients [*Dentz et al.*, 2003].

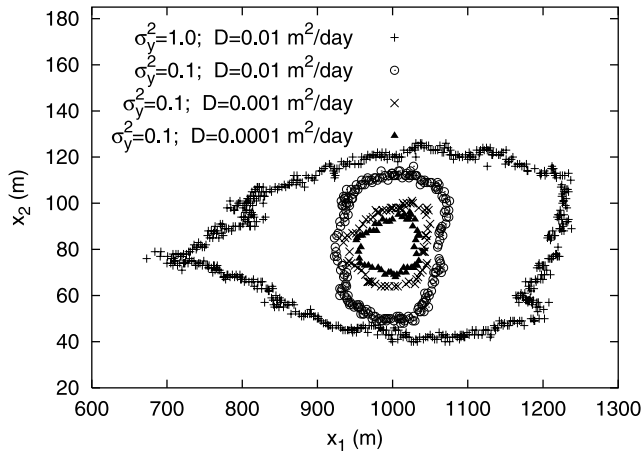


Figure B1. Diffusion fronts at $t = 1000$ days.

[60] The averages of the effective coefficients, over 256 realizations of the velocity, for fixed $\sigma_y^2 = 0.1$ and three different values of the local dispersion coefficients ($D = 0.01 \text{ m}^2/\text{d}$, $D = 0.001 \text{ m}^2/\text{d}$, and $D = 0.0001 \text{ m}^2/\text{d}$ respectively) are presented in Figures B2 and B3 as functions of time and the corresponding Péclet numbers $Pe = U\lambda_y/D$. The comparisons from Figures B2 and B3 show that besides the small asymmetry shown in Figure B1, the increase of Pe considerably increases the time necessary to reach the asymptotic coefficients D_{11}^* (horizontal lines in Figures B2 and B3).

B2. Number of Periods Np , the Number of Realizations R and the Correlation Shape

[61] The periodic fields generated with the Kraichnan algorithm approximate Gaussian fields for $Np \rightarrow \infty$. While ensemble averages are well approximated for tens of periods Np in the Kraichnan routine [Jaekel and Vereecken, 1997; Schwarze et al., 2001], to approximate fluctuations much larger Np are necessary [Eberhard, 2004]. To assess the value of Np we compared the fluctuations of the cross-section concentration and of the longitudinal effective coefficient (defined as in section 4). We considered a point

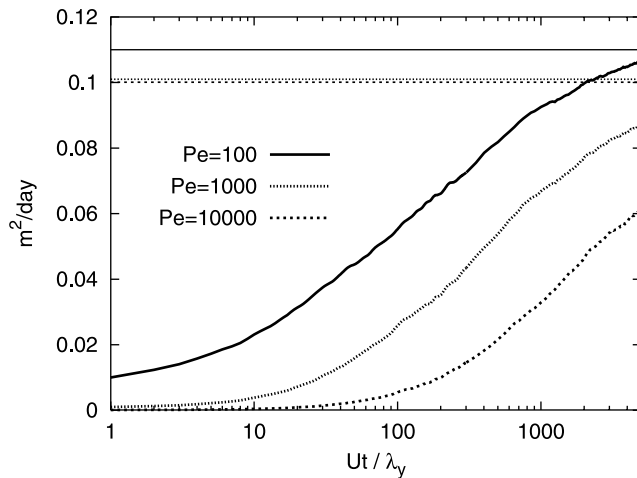


Figure B2. Longitudinal ensemble averaged effective coefficient $\langle D_{11}^{\text{eff}} \rangle$ for different Péclet numbers.

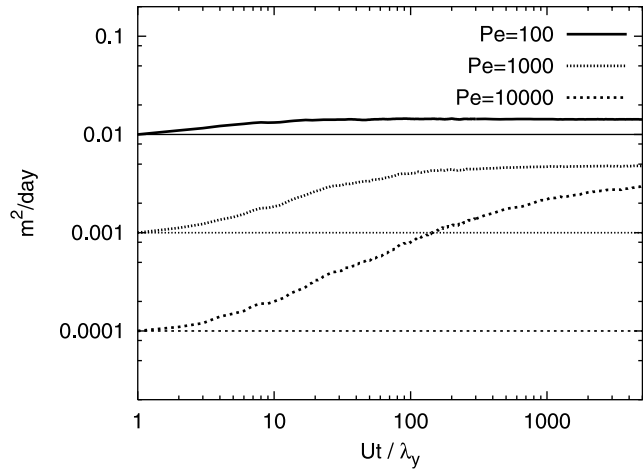


Figure B3. Transverse ensemble averaged effective coefficient $\langle D_{22}^{\text{eff}} \rangle$ for different Péclet numbers.

source, a fixed number of realizations $R = 1024$, exponential and Gaussian shape of the correlation of the log hydraulic conductivity, with the same $\lambda_y = 1 \text{ m}$ and $\sigma_y^2 = 0.1$. The results presented in Figures B4 and B5 suggest that Np must be at least as large as the total number of time steps in simulations. (The fluctuations of the transverse coefficient, not presented here, are already reliable for $Np = 64$.) Therefore, for times up to $t = 4000\lambda_y/U$, we used $Np = 6400$ to approximate the behavior of the transport in Gaussian velocity fields.

[62] Figure B6 presents the fluctuations of the longitudinal effective coefficient for fixed $Np = 6400$ and increasing number of realizations R , in the case of exponential correlation of the log hydraulic conductivity. The increase of R from 256 to 1024 has little influence on the time behavior of the fluctuations. We also found that $R = 256$ ensures the statistical reliability for all the quantities investigated in this study.

B3. Velocity Statistics

[63] In most of numerical studies on the stochastic model [Chin and Wang, 1992; Bellin et al., 1992; Salandin and

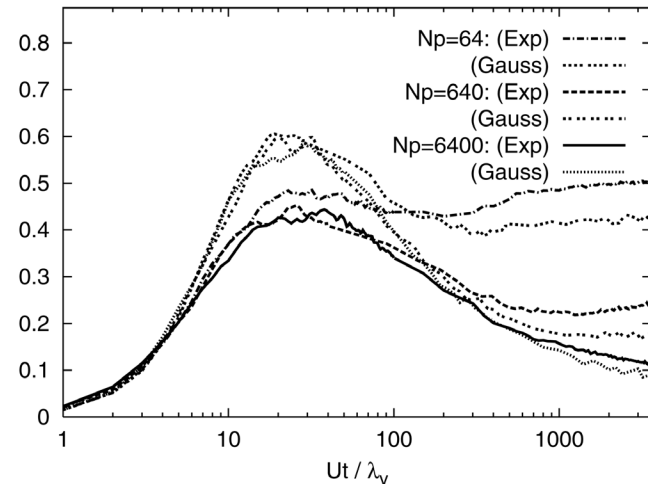


Figure B4. Concentration fluctuations at the plume center of mass for $R = 1024$ and different Np .

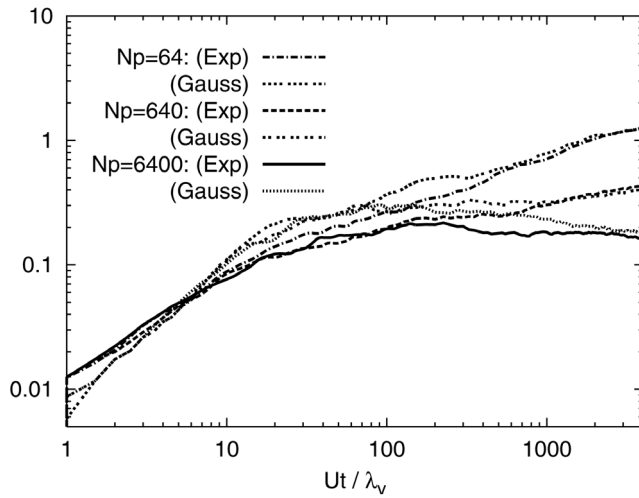


Figure B5. Fluctuations of the longitudinal effective coefficient for $R = 1024$ and different Np .

[Fiorotto, 1998; Naff *et al.*, 1998a; Hassan *et al.*, 1998] the Eulerian statistics of the numerically generated velocity fields was estimated, under the implicit assumption of statistical homogeneity, by space averages in given realizations followed by averages over realizations. This procedure usually underestimates the true statistical parameters. To show that, let us consider the components of the velocity fluctuation $u_l(\mathbf{x}) = V_l(\mathbf{x}) - U_l$, $l = 1, 2$, supposed to be statistically homogeneous variables, and the arithmetic mean over P space points $\langle u_l(\mathbf{x}_p) \rangle_P = \frac{1}{P} \sum_{p=1}^P u_l(\mathbf{x}_p)$. Because the realizations of the velocity computed at different space points belong to the same statistical ensemble, the order of the space and ensemble averages can be interchanged and due to the statistical homogeneity, we have the relations $\langle \langle u_l \rangle_P \rangle = \langle \langle u_l \rangle_P \rangle = \langle u_l \rangle = 0$ and $\langle \langle u_l^2 \rangle_P \rangle = \langle \langle u_l^2 \rangle_P \rangle = \langle u_l^2 \rangle$. The average over realizations of the variance defined through space averages,

$$\langle \langle u_l^2 \rangle_P \rangle - \langle u_l \rangle_P^2 = \langle u_l^2 \rangle - \langle \langle u_l \rangle_P \rangle^2,$$

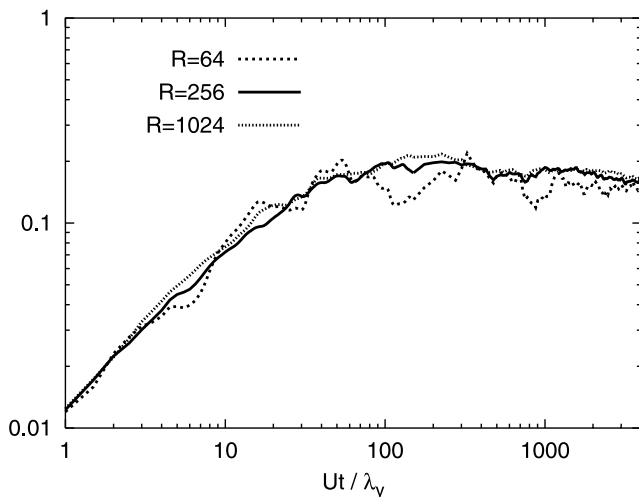


Figure B6. Fluctuations of the longitudinal effective coefficient for $Np = 6400$ and different R .

underestimates the true variance $\sigma_{ul}^2 = \langle u_l^2 \rangle$ of the homogeneous variable u_l with the term $\langle \langle u_l \rangle_P^2 \rangle$, which is the variance of the space mean $\langle u_l \rangle_P$. The last quantity vanishes only when the space mean equals the ensemble mean $\langle u_l \rangle_P = \langle u_l \rangle = 0$. The numerical fields have poor ergodic properties and, as already noted by Bellin *et al.* [1992], they are not strictly statistically homogeneous. Therefore the statistical properties of the numerical velocity fields should be investigated through ensemble averages followed by space averages. This procedure allows the estimation of the non-homogeneity. For instance, the mean velocity $\langle u_l \rangle$ is estimated through space averages $\langle \langle u_l \rangle_P \rangle$ with the standard error of the mean given by

$$\sqrt{\frac{\langle \langle u_l \rangle_P^2 \rangle - \langle \langle u_l \rangle_P \rangle^2}{P-1}}.$$

In our present numerical investigations we used such standard errors to estimate the precision for the velocity moments.

[64] Using 512 velocity values generated by Kraichnan routine, at 512 different space points inside a square the side of which was $10 \lambda_y$, the velocity probability densities were found to be very close to Gaussian homogeneous distributions. The first three moments of the longitudinal and transverse velocity are presented in Table B1. The first and third moment are close to zero. The longitudinal and transverse variances (the second row in Table B1) are respectively $\simeq \frac{3}{8} \sigma_y^2$ and $\simeq \frac{1}{8} \sigma_y^2$, in agreement with the first order asymptotic expansions of the Darcy and the continuity equations [Dagan, 1984].

[65] The velocity correlations

$$r_{ll}(x) = \langle \langle u_l(x_{01}, x_{02}) u_l(x_{01} + x, x_{02}) \rangle \rangle_P, \quad l = 1, 2,$$

were computed as averages over 512 realizations of the velocity and over $P = 11011$ points (x_{01}, x_{02}) (all the grid points in a band of $\lambda_y \times 100\lambda_y$, which corresponds to the largest initial plume in the present simulations). The integrals of the correlation functions r_{ll} give the numerical estimation of the second terms in (4), which describe the contribution of the velocity fluctuations to the upscaled diffusion coefficients,

$$J_{ll}(t) = \int_0^t r_{ll}(U t') dt' = \frac{1}{U} \int_0^{Ut} r_{ll}(x) dx.$$

The numerical integrations between 0 and $t = 5000 \lambda_y / U$ of the correlation functions are presented in Figure B7. The values of J_{ll} are close to the theoretical values (6), $J_{11}^* = D_{11}^* - D = 0.1 \text{ m}^2/\text{d}$ and $J_{22}^* = D_{22}^* - D = 0 \text{ m}^2/\text{d}$. Because the correlations computed by ensemble averages $\langle u_l(x_{01}, x_{02}) u_l(x_{01} + x, x_{02}) \rangle$ differ from point to point, i.e., the random field is not

Table B1. First Three Moments of the Longitudinal and Transverse Velocity Components

	$l = 1$	$l = 2$
$\langle \langle u_l \rangle_P \rangle$	0.00214 ± 0.00033	-0.00051 ± 0.00021
$\langle \langle (u_l - \langle u_l \rangle_P)^2 \rangle_P \rangle$	0.03801 ± 0.00010	0.01268 ± 0.00004
$\langle \langle (u_l - \langle u_l \rangle_P)^3 \rangle_P \rangle$	-0.00014 ± 0.00003	0.00000 ± 0.00001

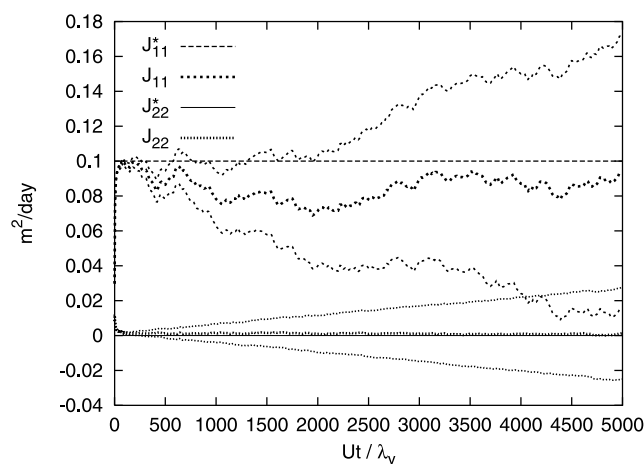


Figure B7. Progress of the time integral of the velocity correlation functions along with mean values and confidence intervals.

strictly homogeneous, at large distances the upper estimate of r_{II} (i.e., space mean plus standard error) is mainly positive and the lower estimate mainly negative. As a direct consequence, the confidence intervals of J_{II} grow linearly with x (see thin lines in Figure B7). Since the standard errors decrease as $(P - 1)^{-1/2}$, reliable estimations of the upscaled effective dispersion coefficients require averaging over large space domains. This remark is valid not only in the case of numerical fields generated by the Kraichnan algorithm but also for all large-scale numerical simulations, where the accumulation of the numerical errors can result in large uncertainty of the numerical estimations.

[66] **Acknowledgments.** The research reported in this paper was supported in part by the Deutsche Forschungsgemeinschaft grant SU 415/1-1, awarded to the first author. Part of the work is a contribution to the “Interdisciplinary Programme for the Prevention of the Major Risk Phenomena at National Level” of the Romanian Academy. The computations on the Jump supercomputer at Research center Jülich were done in cooperation with the John von Neumann Institute for Computing in the frame of project JICG41. The authors are grateful to U. Jaekel, M. Dentz, H. Schwarze, J. P. Eberhard, and A. Engler for their comments on an earlier version of the manuscript and to three anonymous reviewers for constructive remarks. They also acknowledge the technical assistance during the computations offered by J. Heidbüchel and P. Ustohal.

References

- Ababou, R., D. McLaughlin, L. W. Gelhar, and A. F. B. Thompson (1989), Numerical simulation of three-dimensional saturated flow in randomly heterogeneous porous media, *Transp. Porous Media*, 4, 549–565.
- Attinger, S., M. Dentz, H. Kinzelbach, and W. Kinzelbach (1999), Temporal behavior of a solute cloud in a chemically heterogeneous porous medium, *J. Fluid Mech.*, 386, 77–104.
- Avellaneda, M., and M. Majda (1989), Stieltjes integral representation and effective diffusivity bounds for turbulent diffusion, *Phys. Rev. Lett.*, 62(7), 753–755.
- Avellaneda, M., and M. Majda (1992), Superdiffusion in nearly stratified flows, *J. Stat. Phys.*, 69(3/4), 689–729.
- Bellin, A., P. Salandin, and A. Rinaldo (1992), Simulation of dispersion in heterogeneous porous formations: Statistics, first-order theories, convergence of computations, *Water Resour. Res.*, 28(9), 2211–2227.
- Berkowitz, B. (2001), Dispersion in heterogeneous geological formations: Preface, *Transp. Porous Media*, 42, 1–2.
- Berkowitz, B., and H. Scher (2001), Probabilistic approaches to transport in heterogeneous media, *Transp. Porous Media*, 42, 241–263.
- Chin, D. A., and T. Wang (1992), An investigation of the validity of first-order stochastic dispersion theories in isotropic porous media, *Water Resour. Res.*, 28(6), 1531–1542.

- Clinchy, M., and H. Kinzelbach (2001), Stratified disordered media: Exact solutions for transport parameters and their self-averaging properties, *J. Phys. A Math. Gen.*, 34, 7142–7152.
- Cortis, A., H. Scher, and B. Berkowitz (2004), Numerical simulation of non-Fickian transport in geological formations with multiple-scale heterogeneity, *Water Resour. Res.*, 40, W04209, doi:10.1029/2003WR002750.
- Cushman, J. H., and M. Moroni (2001), Statistical mechanics with three-dimensional particle tracking velocimetry experiments in the study of anomalous dispersion. I. Theory, *Phys. Fluids*, 13(1), 75–80.
- Dagan, G. (1984), Solute transport in heterogeneous porous formations, *J. Fluid Mech.*, 145, 151–177.
- Dagan, G. (1987), Theory of solute transport by groundwater, *Water Resour. Res.*, 19, 183–215.
- Dagan, G. (1990), Transport in heterogeneous porous formations: Spatial moments, ergodicity, and effective dispersion, *Water Resour. Res.*, 26, 1281–1290.
- Dagan, G. (2004), Comment on “Exact averaging of stochastic equations for transport in random velocity field,” *Transport in Porous Media*, 50, 223–241, 2003, and “Probability density functions for solute transport in random field,” *Transport in Porous Media*, 50, 243–266, 2003, *Transp. Porous Media*, 55, 113–116.
- Dagan, G., and A. Fiori (1997), The influence of pore-scale dispersion on concentration statistical moments in transport through heterogeneous aquifers, *Water Resour. Res.*, 33, 1595–1607.
- Dentz, M., H. Kinzelbach, S. Attinger, and W. Kinzelbach (2000a), Temporal behavior of a solute cloud in a heterogeneous porous medium: 1. Point-like injection, *Water Resour. Res.*, 36, 3591–3604.
- Dentz, M., H. Kinzelbach, S. Attinger, and W. Kinzelbach (2000b), Temporal behavior of a solute cloud in a heterogeneous porous medium 2. Spatially extended injection, *Water Resour. Res.*, 36, 3605–3614.
- Dentz, M., H. Kinzelbach, S. Attinger, and W. Kinzelbach (2002), Temporal behavior of a solute cloud in a heterogeneous porous medium: 3. Numerical simulations, *Water Resour. Res.*, 38(7), 1118, doi:10.1029/2001WR000436.
- Dentz, M., H. Kinzelbach, S. Attinger, and W. Kinzelbach (2003), Numerical studies of the transport behavior of a passive solute in a two-dimensional incompressible random flow field, *Phys. Rev. E*, 67, 046306.
- Eberhard, J. (2004), Approximations for transport parameters and self-averaging properties for point-like injections in heterogeneous media, *J. Phys. A Math. Gen.*, 37, 2549–2571.
- Fernández-García, D., T. H. Illangasekare, and H. Rajaram (2005a), Differences in the scale dependence of dispersivity and retardation factors estimated from forced-gradient and uniform flow tracer tests in three-dimensional physically and chemically heterogeneous porous media, *Water Resour. Res.*, 41, W03012, doi:10.1029/2004WR003125.
- Fernández-García, D., H. Rajaram, and T. H. Illangasekare (2005b), Assessment of the predictive capabilities of the stochastic theories in a three-dimensional laboratory test aquifer: Effective hydraulic conductivity and temporal moments of breakthrough curves, *Water Resour. Res.*, 41, W04002, doi:10.1029/2004WR003523.
- Fiori, A. (1996), Finite Peclet extensions of Dagan’s solutions to transport in anisotropic heterogeneous formations, *Water Resour. Res.*, 32, 193–198.
- Fiori, A. (1998), On the influence of pore-scale dispersion in nonergodic transport in heterogeneous formations, *Transp. Porous Media*, 30, 57–73.
- Fiori, A., and G. Dagan (2000), Concentration fluctuations in aquifer transport: A rigorous first-order solution and applications, *J. Contam. Hydrol.*, 45, 139–163.
- Fiori, A., I. Janković, and G. Dagan (2003), Flow and transport in highly heterogeneous formations: 2. Semianalytical results for isotropic media, *Water Resour. Res.*, 39(9), 1269, doi:10.1029/2002WR001719.
- Hassan, A. H., J. H. Cushman, and J. W. Delleur (1998), A Monte Carlo assessment of Eulerian flow and transport perturbation models, *Water Resour. Res.*, 34(5), 1143–1163.
- Jaekel, U., and H. Vereecken (1997), Renormalization group analysis of macrodispersion in a directed random flow, *Water Resour. Res.*, 33, 2287–2299.
- Janković, I., A. Fiori, and G. Dagan (2003), Flow and transport in highly heterogeneous formations: 3. Numerical simulations and comparison with theoretical results, *Water Resour. Res.*, 39(9), 1270, doi:10.1029/2002WR001721.
- Kabala, Z. J., and G. Sposito (1994), Statistical moments of reactive solute concentration in a heterogeneous aquifer, *Water Resour. Res.*, 30, 759–768.
- Kapoor, C., and L. W. Gelhar (1994), Transport in three-dimensionally heterogeneous aquifers: 1. Dynamics of concentration fluctuations, *Water Resour. Res.*, 30(6), 1775–1788.

- Kapoor, C., and P. K. Kitanidis (1998), Concentration fluctuation and dilution in aquifers, *Water Resour. Res.*, **34**, 1181–1193.
- Kesten, H., and G. C. Papanicolaou (1979), A limit theorem for turbulent diffusion, *Commun. Math. Phys.*, **65**, 97–128.
- Kitanidis, P. K. (1988), Prediction by the method of moments of transport in a heterogeneous formation, *J. Hydrol.*, **102**, 453–473.
- Kraichnan, R. H. (1970), Diffusion by a random velocity field, *Phys. Fluids*, **13**(1), 22–31.
- Kurbanmuradov, O., K. Sabelfeld, O. F. Smidts, and H. Vereecken (2003), A Lagrangian stochastic model for the transport in statistically homogeneous porous media, *Monte Carlo Methods Appl.*, **9**(4), 341–366.
- Labolle, E. M., and G. Fogg (2001), Role of molecular diffusion in contaminant migration and recovery in an alluvial aquifer system, *Transp. Porous Media*, **42**, 155–179.
- Matheron, G., and G. de Marsily (1980), Is transport in porous media always diffusive?, *Water Resour. Res.*, **16**, 901–917.
- Moltyaner, G. L., M. H. Klukas, C. A. Willis, and R. W. D. Killey (1993), Numerical simulations of Twin Lake natural-gradient tracer tests: A comparison of methods, *Water Resour. Res.*, **29**(10), 3433–3452.
- Naff, R. L., D. F. Haley, and E. A. Sudicky (1998a), High-resolution Monte Carlo simulation of flow and conservative transport in heterogeneous porous media: 1. Methodology and flow results, *Water Resour. Res.*, **34**(4), 663–677.
- Naff, R. L., D. F. Haley, and E. A. Sudicky (1998b), High-resolution Monte Carlo simulation of flow and conservative transport in heterogeneous porous media: 2. Transport results, *Water Resour. Res.*, **34**(4), 679–697.
- Pannone, M., and P. K. Kitanidis (1999), Large time behavior of concentration variance and dilution in heterogeneous formations, *Water Resour. Res.*, **35**(3), 623–634.
- Rajaram, H., and L. W. Gelhar (1993a), Plume scale-dependent dispersion in heterogeneous aquifers: 1. Lagrangian analysis in a stratified aquifer, *Water Resour. Res.*, **29**, 3249–3260.
- Rajaram, H., and L. W. Gelhar (1993b), Plume scale-dependent dispersion in heterogeneous aquifers: 2. Eulerian analysis and three-dimensional aquifers, *Water Resour. Res.*, **29**, 3261–3276.
- Roth, K., and K. Hammel (1996), Transport of conservative chemical through an unsaturated two-dimensional Miller-similar medium with steady state flow, *Water Resour. Res.*, **32**, 1653–1663.
- Salandin, P., and V. Fiorotto (1998), Solute transport in highly heterogeneous aquifers, *Water Resour. Res.*, **34**, 949–961.
- Schwarze, H., U. Jaekel, and H. Vereecken (2001), Estimation of macrodispersivity by different approximation methods for flow and transport in randomly heterogeneous media, *Transp. Porous Media*, **43**, 265–287.
- Smith, L., and F. W. Schwartz (1980), Mass transport: 1. A stochastic analysis of macroscopic dispersion, *Water Resour. Res.*, **16**, 303–313.
- Sposito, G. (1997), Ergodicity and the “scale effect”, *Adv. Water Resour.*, **20**, 309–316.
- Sposito, G. (2001), Topological groundwater hydrodynamics, *Adv. Water Resour.*, **24**, 793–801.
- Sposito, G., and G. Dagan (1994), Predicting solute plume evolution in heterogeneous porous formations, *Water Resour. Res.*, **30**(2), 585–589.
- Sposito, G., W. A. Jury, and V. K. Gupta (1986), Fundamental problems in the stochastic convection-dispersion model of solute transport in aquifers and field soils, *Water Resour. Res.*, **22**, 77–88.
- Suciu, N., C. Vamoş, H. Vereecken, and J. Vanderborght (2002), Numerical modeling of solute transport in heterogeneous aquifers and self-averaging, in *Proceedings of the first Workshop on Mathematical Modeling of Environmental Problems*, edited by G. Marinovschi and I. Stelian, pp. 111–140, Rom. Acad. Publ. House, Bucharest.
- Suciu, N., C. Vamoş, J. Vanderborght, H. Hardelauf, and H. Vereecken (2004), Numerical modeling of large scale transport of contaminant solutes using the global random walk algorithm, *Monte Carlo Methods Appl.*, **10**(2), 153–177.
- Suciu, N., C. Vamoş, P. Knabner, and U. Rüde (2005), Biased global random walk, a cellular automaton for diffusion, in *Simulationstechnique, 18th Symposium in Erlangen, September 2005*, edited by F. Hülsemann, M. Kowarschik, and U. Rüde, pp. 562–567, SCS Publ. House, Erlangen, Germany.
- Sun, N.-Z. (1996), *Mathematical Modeling in Groundwater Pollution*, Springer, New York.
- Tatarinova, E. B., P. A. Kalugin, and A. V. Sokol (1991), What is the propagation rate of the passive component in turbulent flow limited by?, *Europhys. Lett.*, **14**(8), 773–777.
- Taylor, G. I. (1921), Diffusion by continuous movements, *Proc. London Math. Soc.*, **2**(20), 196–212.
- Tompson, A. F. B., and L. W. Gelhar (1990), Numerical simulation of solute transport in three-dimensional, randomly heterogeneous porous media, *Water Resour. Res.*, **26**(10), 2541–2562.
- Trefry, M. G., F. P. Ruan, and D. McLaughlin (2003), Numerical simulations of preasymptotic transport in heterogeneous porous media: Departures from the Gaussian limit, *Water Resour. Res.*, **39**(3), 1063, doi:10.1029/2001WR001101.
- Vamoş, C., N. Suciu, and H. Vereecken (2003), Generalized random walk algorithm for the numerical modeling of complex diffusion processes, *J. Comput. Phys.*, **186**(2), 527–544.
- Vanderborght, J., and H. Vereecken (2002), Estimation of local scale dispersion from local breakthrough curves during a tracer test in a heterogeneous aquifer: The Lagrangian approach, *J. Contam. Hydrol.*, **54**, 141–171.
- Winter, C. L., C. M. Newman, and S. P. Neuman (1984), A perturbation expansion for diffusion in random velocity field, *SIAM J. Appl. Math.*, **44**(2), 411–424.
- Zhang, Y.-K., and J. Lin (1998), Numerical simulations of transport of nonergodic solute plumes in heterogeneous aquifers, *Stochastic Hydrol. Hydrol.*, **12**(2), 117–139.
- Zhang, Y.-K., and B.-M. Seo (2004), Stochastic analyses and Monte Carlo simulations of nonergodic solute transport in three-dimensional heterogeneous statistically anisotropic aquifers, *Water Resour. Res.*, **40**, W05103, doi:10.1029/2003WR002871.
- Zhang, Y.-K., and D. Zhang (1997), Time-dependent dispersion of nonergodic plumes in two-dimensional heterogeneous aquifers, *J. Hydrol. Eng.*, **2**(2), 91–94.
- Zhang, Y.-K., D. Zhang, and J. Lin (1996), Nonergodic solute transport in three-dimensional heterogeneous isotropic aquifers, *Water Resour. Res.*, **32**(9), 2955–2963.

H. Hardelauf, J. Vanderborght, and H. Vereecken, Institute of Agrosphere (IGC-IV), Research Center Jülich, D-52425 Jülich, Germany.

N. Suciu, Institute of Applied Mathematics, Friedrich-Alexander University of Erlangen-Nuremberg, Martensstrasse 3, D-91058 Erlangen, Germany. (suciu@am.uni-erlangen.de)

C. Vamoş, “T. Popoviciu” Institute of Numerical Analysis, Romanian Academy, P.O. Box 68-1, 400320 Cluj-Napoca, Romania.